

## Supporting Information

# Charge-Regulated Fluorescent Anchors Enable High-Fidelity Tracking of Plasma Membrane Dynamics During Biological Events

Jiaqi Zuo,<sup>†a</sup> Aohui Peng,<sup>†b</sup> Penglei Wu,<sup>a</sup> Junyi Chen,<sup>b</sup> Chuangye Yao,<sup>a</sup> Junjun Pan,<sup>a</sup> Engao Zhu,<sup>b</sup> Yingye Weng,<sup>b</sup> Kewei Zhang,<sup>b</sup> Hui Feng,<sup>a</sup> Zhigang Jin,<sup>b\*</sup> and Zhaosheng Qian<sup>a\*</sup>

<sup>a</sup> Key Laboratory of the Ministry of Education for Advanced Catalysis Materials, College of Chemistry and Materials Science, Zhejiang Normal University, Jinhua 321004, China

<sup>b</sup> College of Life Sciences, Zhejiang Normal University, Jinhua 321004, China

### Table of Contents

#### 1. Materials and Experimental Section.

1.1 Materials.

1.2 Characterization of UV-Visible and Fluorescence Properties of All Samples

1.3 Fluorescence Response of CSP Dyes to DOPC

1.4 Cell culture

1.5 Cell viability assay

1.6 Fluorescence imaging of living cells

1.7 Comparison with commercial membrane dyes

1.8 Cell fusion

1.9 Fluorescence recovery after photobleaching (FRAP)

1.10 *Caenorhabditis elegans* culture and manipulations

1.11 Toxicity Test of CSP-DBO towards *Arabidopsis Thaliana*

1.12 Confocal Imaging of Plasma Membrane of *Arabidopsis Thaliana*

**1.13** Plasmolysis of Onion Epidermal Cells

**1.14** Dynamic Tracking of Plasma Membrane Damage Caused by DMSO

**1.15** Three-Dimensional Imaging of Plasma Membrane of Onion Epidermal Cells

**1.16** The Statistical Data Process Details of Quantitative Analysis

## **2. Synthesis and Characterization of Dyes**

## **3. Supplementary Schemes and Figures**

**Scheme S1.** Synthesis routes of CSP, CSP-TEA, CSP-TPP and CSP-DBO.

**Table S1.** The optical parameters of the dyes used for confocal imaging experiments.

**Figure S1.** (A) Qualitative illustration of the distribution of CSP-TEA, CSP-TPP and CSP-DBO between 1-Octanol containing DOPC (40  $\mu\text{M}$ ) and water. (B) Quantitative lipid-water partition coefficient ( $\log P$ ) of CSP-TEA, CSP-TPP and CSP-DBO.

**Figure S2.** Laser scanning confocal microscopy images of *Arabidopsis thaliana* stained with different amounts of dyes at different staining time. (A) CSP for 2 min: (a, d) 5.0  $\mu\text{M}$ ; (b, e) 10.0  $\mu\text{M}$ ; (c, f) 20.0  $\mu\text{M}$ ; Scale bar = 50  $\mu\text{m}$ . (B) CSP-TPP for 2 min: (a, d) 5.0  $\mu\text{M}$ ; (b, e) 10.0  $\mu\text{M}$ ; (c, f) 20.0  $\mu\text{M}$ ; Scale bar= 5  $\mu\text{m}$  (a, d, c, f), Scale bar= 10  $\mu\text{m}$  (b, e). (C) CSP-TEA for 2 min: (a, d) 5.0  $\mu\text{M}$ ; (b, e) 10.0  $\mu\text{M}$ ; (c, f) 20.0  $\mu\text{M}$ ; Scale bar= 5  $\mu\text{m}$  (a, d), Scale bar= 10  $\mu\text{m}$  (b, e, c, f). (D) CSP-DBO for 2 min: (a, d) 5.0  $\mu\text{M}$ ; (b, e) 10.0  $\mu\text{M}$ ; (c, f) 20.0  $\mu\text{M}$ ; Scale bar= 10  $\mu\text{m}$  (a, d), Scale bar= 5  $\mu\text{m}$  (b, e, c, f).

**Figure S2.** Laser scanning confocal microscopy images in seedling roots of *Arabidopsis thaliana* stained with (A) CSP-DBO (10.0  $\mu\text{M}$  probes incubated for 2 min) (B) CSP-TPP (5.0  $\mu\text{M}$  probes incubated for 2 min) (C) CSP-TEA (10.0  $\mu\text{M}$  probes incubated for 2 min) at various time points. Scale bar = 10  $\mu\text{m}$ .

**Figure S3.** Laser scanning confocal microscopy images in seedling roots tip cells of *Arabidopsis thaliana* stained with CSP-DBO (10.0  $\mu\text{M}$  probes incubated for 2 min). (a) The plasma membrane was labelled with red color in dark field; (b) the vacuoles were observed at the center

of the cells in bright field; (c) in the merged image, no overlap between the plasma membrane and the vacuole was observed. Scale bar = 10  $\mu\text{m}$ .

**Figure S4.** (A) 3D tracking of morphological changes of the plasma membrane in onion epidermal cells stained with CSP-DBO (20  $\mu\text{M}$ ) during water loss process. Scale bar = 50  $\mu\text{m}$ . (B) Z-stack images of onion epidermal cells from 1 to 21.98  $\mu\text{m}$  after staining with CSP-DBO (20  $\mu\text{M}$ ).

**Figure S5.** Laser scanning confocal microscopy images in seedling roots of *Arabidopsis thaliana* stained with (A) CSP-TPP (5.0  $\mu\text{M}$  probes incubated for 2 min) (B) CSP-TEA (10.0  $\mu\text{M}$  probes incubated for 2 min) at various time points. Scale bar = 10  $\mu\text{m}$ .

**Figure S6.** (A) UV-visible spectrum of CSP-DBO (10.0  $\mu\text{M}$ ) in  $\text{H}_2\text{O}$  at various time points via a long-term irradiation (561 nm 20 mW); (B) The change in absorbance of the peak at 513 nm of CSP-DBO (10.0  $\mu\text{M}$ ) in  $\text{H}_2\text{O}$  versus irradiation time by using the excitation source of 561 nm 20 mW.

**Figure S7.** (A) PL spectra of CSP-DBO (10.0  $\mu\text{M}$ ) in  $\text{H}_2\text{O}$  at various time points via a long-term irradiation (561 nm 20 mW); (B) The change of PL spectra of CSP-DBO (10.0  $\mu\text{M}$ ) in  $\text{H}_2\text{O}$  at various time points via a long-term irradiation (561 nm 20 mW).

**Figure S8.** (A) The changes of laser scanning confocal microscopy images in seedling roots of *Arabidopsis thaliana* stained with CSP-DBO (10.0  $\mu\text{M}$ ) for 2 min versus irradiation time at 561 nm using the excitation source of the used microscope: (a) CSP-DBO (0 min); (b) CSP-DBO (15 min); (c) CSP-DBO (30 min); (d) CSP-DBO (45 min); (e) CSP-DBO (60 min); (f) CSP-DBO (75 min); (g) CSP-DBO (90 min). Scale bar = 10  $\mu\text{m}$ . (B) The change of PL intensity of CSP-DBO inserted inside the cell membranes versus irradiation time at 561 nm using the excitation source of the used microscope.

**Figure S9.** (A) Photographs of representative *Arabidopsis thaliana* seedlings incubated without (Mock) and with different concentrations of CSP-DBO (1.0  $\mu\text{M}$  to 50.0  $\mu\text{M}$ ) after 6 days. (b) Average root lengths of *Arabidopsis thaliana*

seedlings incubated without (Mock) and with different concentrations of CSP-DBO (1.0  $\mu$ M to 50.0  $\mu$ M) after 6 days.

**Figure S10.** (A) Change in PL intensity of the CSP-DBO in PBS (20.0  $\mu$ M) versus pH values.  $\lambda_{em}$  = 515 nm; (B) Change in mean PL intensity of the CSP-DBO in PBS (20.0  $\mu$ M) versus pH values by using line charts.  $\lambda_{em}$  = 515 nm.

**Figure S11.** Viability of cancer cell (HeLa) and normal cell (HEK293T) incubated with different concentrations of CSP-DBO (0  $\mu$ M to 30.0  $\mu$ M) and 1 mM H<sub>2</sub>O<sub>2</sub> (positive control) after 24 h.

**Figure S12.** Evaluation of biocompatibility of CSP-DBO in *C. elegans*. (A) The frequency of body bends within 30s; (B) The frequency of head thrashes within 30s.

**Figure S13.** Evaluation the biocompatibility (lifespan) of CSP-DBO in *C. elegans*.

**Figure S14.** Laser scanning confocal microscopy images of *C. elegans* stained with CSP-DBO (a – c:10.0  $\mu$ M, 30min; d – f: 20.0  $\mu$ M, 30min). Scale bar = 50  $\mu$ m.

#### 4. Spectra of Compounds

**Figure S15.** <sup>1</sup>H NMR spectra of N,N-dihexylaniline (1) in CDCl<sub>3</sub>

**Figure S16.** <sup>13</sup>C NMR spectra of N,N-dihexylaniline (1) in CDCl<sub>3</sub>

**Figure S17.** <sup>1</sup>H NMR spectra of 4-(dihexylamino)benzaldehyde (2) in CDCl<sub>3</sub>

**Figure S18.** <sup>13</sup>C NMR spectra of 4-(dihexylamino)benzaldehyde (2) in CDCl<sub>3</sub>

**Figure S19.** <sup>1</sup>H NMR spectra of (Z)-3-(4-(dihexylamino)phenyl)-2-(pyridin-4-yl)acrylonitrile (3) in CDCl<sub>3</sub>

**Figure S20.** <sup>13</sup>C NMR spectra of (Z)-3-(4-(dihexylamino)phenyl)-2-(pyridin-4-yl)acrylonitrile (3) in CDCl<sub>3</sub>

**Figure S21.** <sup>1</sup>H NMR spectra of CSP in CDCl<sub>3</sub>

**Figure S22.** <sup>13</sup>C NMR spectra of CSP in CDCl<sub>3</sub>

**Figure S23.** <sup>1</sup>H NMR spectra of CSP-TEA in CDCl<sub>3</sub>

**Figure S24.** <sup>13</sup>C NMR spectra of CSP-TEA in CDCl<sub>3</sub>

**Figure S25.** <sup>1</sup>H NMR spectra of CSP-TPP in CDCl<sub>3</sub>

**Figure S26.** <sup>13</sup>C NMR spectra of CSP-TPP in CD<sub>3</sub>OD

**Figure S27.** <sup>1</sup>H NMR spectra of CSP-DBO in CD<sub>3</sub>OD

**Figure S28.**  $^{13}\text{C}$  NMR spectra of CSP-DBO in  $\text{CD}_3\text{OD}$

**Figure S29.**  $^1\text{H}$  NMR spectra of 3-bromo-N,N,N-triethylpropan-1-aminium in  $\text{D}_2\text{O}$

**Figure S30.**  $^{13}\text{C}$  NMR spectra of 3-bromo-N,N,N-triethylpropan-1-aminium in  $\text{D}_2\text{O}$

**Figure S31.**  $^1\text{H}$  NMR spectra of (3-bromopropyl)triphenylphosphonium in  $\text{CD}_3\text{OD}$

**Figure S32.**  $^{13}\text{C}$  NMR spectra of (3-bromopropyl)triphenylphosphonium in  $\text{CD}_3\text{OD}$

**Figure S33.**  $^1\text{H}$  NMR spectra of 1-(3-bromopropyl)-1,4-diazabicyclo [2.2.2] octan-1-ium in  $\text{D}_2\text{O}$

**Figure S34.**  $^{13}\text{C}$  NMR spectra of 1-(3-bromopropyl)- 1,4-diazabicyclo[2.2.2] octan-1-ium in  $\text{D}_2\text{O}$

**Figure S35.** High-resolution mass spectrum of N,N-dihexylaniline (1)

**Figure S36.** High-resolution mass spectrum of 4-(dihexylamino)benzaldehyde (2)

**Figure S37.** High-resolution mass spectrum of (Z)-3-(4-(dihexylamino)phenyl)-2-(pyridin-4-yl)acrylonitrile (3)

**Figure S38.** High-resolution mass spectrum of (Z)-4-(1-cyano-2-(4-(dihexylamino)phenyl)vinyl)-1-methylpyridin-1-ium iodide (CSP)

**Figure S39.** High-resolution mass spectrum of (Z)-4-(1-cyano-2-(4-(dihexylamino)phenyl)vinyl)-1-(3-(triethylammonio)propyl)pyridin-1-ium bromide (CSP-TEA)

**Figure S40.** High-resolution mass spectrum of (Z)-4-(1-cyano-2-(4-(dihexylamino)phenyl)vinyl)-1-(3-(triphenylphosphonio)propyl)pyridin-1-ium bromide (CSP-T PP)

**Figure S41.** High-resolution mass spectrum of (Z)-1-(3-(4-(1-cyano-2-(4-dihexylamino)phenyl)vinyl)pyridin-1-ium-1-yl)propyl)-1,4-diazabicyclo[2.2.2]octan-1-ium bromide (CSP-DBO)

**Figure S42.** High-resolution mass spectrum of 3-bromo-N,N,N-triethylpropan-1-ammonium bromide

**Figure S43.** High-resolution mass spectrum of (3-bromopropyl) triphenylphosphonium bromide

**Figure S44.** High-resolution mass spectrum of 1-(3-bromopropyl)-1,4-Diazabicyclo[2.2.2]octan-1-ium bromide

## 5. REFERENCE

## **1. Materials and Experimental Section.**

### **1.1 Materials.**

CellMask Green, DiO, FM 1-43 and DOPC were obtained from commercial sources (*J&K Scientific* and *Thermo Fisher*). HeLa (human cervical cancer cell line), HEK293T (human renal epithelial cell line), chicken erythrocyte (CRBC), and SH-SY5Y (neuroblastoma) were obtained from the American Type Culture Collection or BeNa Culture Collection. All purchased chemicals and reagents are of analytical grade and used without further purification.

### **1.2 Characterization of UV-Visible and Fluorescence Properties of All Samples**

UV-vis absorption spectra were recorded using an Agilent Cary 5000 UV-Vis-NIR spectrophotometer. Steady PL spectra of all samples were performed on an Edinburgh Instruments model FLS980 fluorescence spectrophotometer equipped with a xenon arc lamp using a front face sample holder. Time-resolved fluorescence measurements were conducted with EPL-series lasers.

### **1.3 Fluorescence Response of CSP Dyes to DOPC**

The PL spectrum of each CSP dye in PBS was first recorded, in which the used concentration of each CSP dye was 10  $\mu\text{M}$ . The PL intensity of each CSP dye were measured, which was noted as  $F_{\text{free}}$ . A solution of 1, 2-dioleoyl-sn-glycero-3-phosphocholine (DOPC) with a fixed concentration (100 mg/mL) in triple-distilled water was first prepared, and then added to a corresponding CSP dye solution at 10  $\mu\text{M}$ , resulting in a 5 mg/mL DOPC solution. The PL intensity of each CSP dye bound to DOPC was measured, which was noted as  $F_{\text{bound}}$ . PL spectra were recorded at the corresponding excitation wavelength ( $\lambda_{\text{ex}} = 483 \text{ nm}$  for CSP and CSP-TEA,  $\lambda_{\text{ex}} = 493 \text{ nm}$  for CSP-TPP and CSP-DBO). The PL enhancement ratio was calculated using  $F_{\text{bound}}/F_{\text{free}}$ .

### **1.4 Cell culture**

The human cervical cancer cell line HeLa, the human embryonic kidney cell line HEK293T and the human neuroblastoma cell line SK-N-SH-SY5Y(SH-SY5Y) were routinely cultured at 37°C with 5% CO<sub>2</sub> in Dulbecco's Modified Eagle Medium (DMEM; GENOM, Zhejiang, China), which supplemented with 10% fetal bovine serum (FBS; ExCell Bio, Shanghai, China) and 1% penicillin/streptomycin (Gibco, Gaithersburg, MD).

### **1.5 Cell viability assay**

CSP-DBO was prepared in d<sub>2</sub>H<sub>2</sub>O at a stock concentration of 5mM. Viability of HeLa and HEK293T cells was evaluated by the standard CCK-8 assay following the manufacturer's instructions (MeilunBio, Dalian, China). Briefly, cells grown in log phase were seeded into 96-well plates with density of 1×10<sup>4</sup> cells/well and allowed to adhere for 24 h. CSP-DBO with indicated final concentration, d<sub>2</sub>H<sub>2</sub>O or 1mM H<sub>2</sub>O<sub>2</sub> as the positive control of cytotoxicity was added into cells. 24 h later, the CCK-8 assay were performed and the optical density (OD) at 450 nm was measured using iMark microplate reader (Bio-Rad, Hercules, CA). Each group of the experiment was repeated in triplicate.

### **1.6 Fluorescence imaging of living cells**

CSP and CSP-DBO were prepared in d<sub>2</sub>H<sub>2</sub>O at a stock concentration of 5 mM. CSP-TPP and CSP-TEA were prepared in dimethyl sulfoxide (DMSO; Thermo Fisher, Waltham, MA) at a stock concentration of 50mM. HeLa, HEK293T and SH-SY5Y cells were seeded in 35 mm glass bottom dishes (Cellvis, Sunnyvale, CA) and allowed to adhere for 24 h. After washing with phosphate-buffered saline (PBS) for three times, cells were treated with 10 μM dye in PBS at room temperature for 5 min and then washed with PBS. Fluorescent images of living cells were acquired with Zeiss LSM880 confocal microscopy system with the excitation wavelength at 561 nm.

### **1.7 Comparison with commercial membrane dyes**

To compare the performance of CSP-DBO with commercial membrane dyes, DiO (J&K Scientific, Beijing, China) and CellMask (Thermo Fisher)

plasma membrane stains (green) were used to perform co-staining and real-time tracing of living cells. For co-staining assay, HeLa cells were seeded in 35 mm glass bottom dishes. 24 h later, cells were treated with 5  $\mu\text{M}$  DiO or 5  $\mu\text{g}/\text{mL}$  CellMask for 5 min and washed with PBS for three times. Then cells were treated with 20  $\mu\text{M}$  CSP-DBO for 5 min and washed with PBS to remove the dye. DiO/CSP-DBO or CellMask/CSP-DBO co-stained cells were imaged with Zeiss LSM880 confocal microscope system with the excitation wavelength of DiO and CellMask at 488 nm, and the excitation wavelength of CSP-DBO at 561 nm. For real-time tracing of membrane dyes, HeLa cells were treated with 5  $\mu\text{M}$  DiO, 5  $\mu\text{g}/\text{mL}$  CellMask or 20  $\mu\text{M}$  CSP-DBO for 5 min and washed with PBS. Fluorescent signals in living cells were real-time tracked with Zeiss LSM880 confocal microscope system.

### **1.8 Cell fusion**

After 1 mL cell suspension of 1% chicken erythrocyte (ZEWEIL, Nanjing, China) was preheated in a water bath at 37°C for 1 min, 0.5 mL preheated 50% PEG3350 (Solarbio, Beijing, China) was slowly added to cells suspension and incubated at 37°C for 2min. Cell suspension untreated with PEG3350 was used as negative control of cell fusion. 10  $\mu\text{L}$  of 20  $\mu\text{M}$  CSP-DBO and 10  $\mu\text{L}$  of cell suspension were mixed in a glass slide. The images of fused cells were acquired with Zeiss LSM880 confocal microscope system.

### **1.9 Fluorescence recovery after photobleaching (FRAP)**

CSP-DBO was applied to investigate the dynamics of membrane lipids by using the FRAP module of the Zeiss LSM880 confocal microscopy system as described previously.<sup>[1]</sup> Briefly, HeLa cells in 35 mm glass bottom dishes were treated with 20 $\mu\text{M}$  CSP-DBO for 5 min. A rectangular region of plasma membrane with fluorescent signals emitted by CSP-DBO was bleached 3000 times (each of a short duration) with 561nm and 405nm laser beams with a light intensity of 100%. After photobleaching, time-lapse images were captured every 3s. The fluorescence intensity of pre-bleaching was set to 100%



and the normalized fluorescence intensity at each time point ( $I_t$ ) was used to calculate the recovery index according to the following formula:  $FR(t) = I_t/I_{pre-bleaching}$ . GraphPad Prism was used to plot and analyze the FRAP data.

### **1.10 *Caenorhabditis elegans* culture and manipulations**

*E. coli* OP50 and *C. elegans* wild-type strain N<sub>2</sub> were purchased from the Caenorhabditis Genetics Center (CGC, University of Minnesota, MN). For maintaining the *C. elegans* strain, worms were cultured at 20°C on a nematode growth medium (NGM) agar plate covered with a bacterial lawn of *E. coli* OP50. Hermaphrodites of *C. elegans* were age-synchronized by isolating eggs and incubated for 24 h till to the first larval (L1) stage, and then transferred to NGM plates seeded with *E. coli* OP50 and allowed to further develop into the L4 stage.

To evaluate the biocompatibility of CSP-DBO *in vivo*, approximately 15 L1 worms per group were placed in NGM agar plate and exposed to various concentrations of CSP-DBO (0, 10, 20, 40 μM) for 5 days till to the stage of adult. Neurotoxicity on locomotion behaviors was determined by the frequency of body bends and head thrashes counted within 30 s with a stereo microscope (Motic SMZ-168, Xiamen, China). The effect of CSP-DBO on *C. elegans* lifespan was additionally evaluated. Thirty *C. elegans* at the L4 stage were transferred to NGM agar plates with different concentrations of DBO (0, 20 μM). Six Petri dishes were incubated in each group, and the number of live and dead *C. elegans* were recorded. The surviving *C. elegans* were transferred to new dishes every day. The number of days until all the *C. elegans* died was the life cycle.

To explore imaging performance of CSP-DBO *in vivo*, L4 worms were directly or indirectly stained with CSP-DBO. For direct staining, L4 worms were incubated with 40 μM CSP-DBO in M9 buffer for 30min and washed three times with M9 buffer. For indirect staining, worms of different periods were cultured on NGM agar plate seeded with *E. coli* OP50 and 1 μM CSP-

DBO for 24 h. Approximately 15 worms were anaesthetised by picking them into 35 mm glass bottom dishes containing 5 mM levamisole hydrochloride solution (Sangon, Shanghai, China). Images of stained worms were acquired with Zeiss LSM880 confocal microscope system.

### **1.11 Toxicity Test of CSP-DBO towards *Arabidopsis Thaliana***

The wild-type (Col-0) seeds of *Arabidopsis thaliana* were surface sterilized and imbibed for 3 days at 4°C in dark and then sown onto 0.5×Murashige & Skoog (MS) 1.5% (w/v) agar plates. Seedlings were vertically grown on plates in a climate-controlled growth room (22 / 20 °C day / night temperature, 16 / 8 h photoperiod, and 80  $\mu\text{mol}\cdot\text{s}^{-1}\cdot\text{m}^{-2}$  light intensity). The first group of *Arabidopsis thaliana* was grown under the preceding normal conditions as the control group. The other five groups of *Arabidopsis thaliana* were grown on 0.5 × Murashige & Skoog (MS) 1.5% (w/v) agar plates containing CSP-DBO with different concentrations (1  $\mu\text{M}$ , 5  $\mu\text{M}$ , 10  $\mu\text{M}$ , 20  $\mu\text{M}$  and 50  $\mu\text{M}$ ). The resulting phenotype of two groups was recorded using a camera.

### **1.12 Confocal Imaging of Plasma Membrane of *Arabidopsis Thaliana***

The wild-type (Col-0) seeds of *Arabidopsis thaliana* were surface sterilized and imbibed for 3 days at 4°C in dark and then sown onto 0.5×Murashige & Skoog (MS) 1.5% (w/v) agar plates. Seedlings were vertically grown on plates in a climate-controlled growth room (22/20 °C day / night temperature, 16/8 h photoperiod, and 80  $\mu\text{mol}\cdot\text{s}^{-1}\cdot\text{m}^{-2}$  light intensity). Five-day-old seedlings with healthy roots were used in this study unless otherwise specified. 1/2 MS culture medium and stock solutions of the dyes in H<sub>2</sub>O (20.0 mM) were prepared. After that, 1  $\mu\text{L}$  stock solution of each CSP dye was added to 2 mL 1/2 MS culture medium to get a final staining dye concentration of 10.0  $\mu\text{M}$ . The *Arabidopsis thaliana* seedlings were incubated with each CSP dye for 2 min at 22 °C. Confocal imaging experiments were performed on a Zeiss LSM 880 model confocal laser scanning microscope (Germany) with an excitation at 561 nm.

The optimal concentration and staining time of each CSP dye were optimized using the following steps. The root tip of *Arabidopsis thaliana* was placed in a solution of CSP-DBO with varying concentrations (5.0, 10.0 and 20.0  $\mu\text{M}$ ) for 2 min at 22°C, and then the slide glass with *Arabidopsis thaliana* root tip cells were placed for the following imaging experiments. Fluorescence imaging experiments were performed on a Zeiss LSM 880 model confocal laser scanning microscope (Germany) with an excitation at 561 nm. The same optimal experiments were performed for CSP, CSP-TPP and CSP-TEA.

Long-term imaging experiments of *Arabidopsis thaliana* cells were performed according to the following procedure. The root tip of *Arabidopsis thaliana* was incubated in 2 mL of MS culture containing 10.0  $\mu\text{M}$  CSP-DBO for 2 min, and then was placed between two slide glasses to ensuring long-time stability during imaging. Confocal images of *Arabidopsis thaliana* root tip cells stained with CSP-DBO were collected every 10 min for a total period of 90 minutes under optimal conditions.

During the photostability experiment, the confocal images of root cells of *Arabidopsis thaliana* stained with CSP-DBO was directly recorded in a normal mode at varied time points. The root tip cells were first incubated with CSP-DBO (10.0  $\mu\text{M}$ ) for 2 min, and then continuously irradiated at 561 nm in the range of 0 – 90 min. The confocal images of root cells of *Arabidopsis thaliana* stained with CSP-DBO were recorded during this period with the interval of 10 min, and fluorescence signal intensity from stained cells was continuously monitored and further analyzed.

### **1.13 Plasmolysis of Onion Epidermal Cells**

To evaluate the staining specificity of the CSP dyes to plasma membrane, plasmolysis experiments were conducted as follows. A piece of onion internal epidermis from fresh onion was incubated in a NaCl solution (0.3 g/mL) containing a certain concentration of dyes for a fixed time, during which the staining and plasmolysis were simultaneously achieved. The used

concentration of CSP, CSP-TPP, CSP-TEA and CSP-DBO was 10.0  $\mu\text{M}$  to ensure the image quality, and the staining time was 10 min. Then the confocal images were recorded in a normal mode after plasmolysis.

#### **1.14 Dynamic Tracking of Plasma Membrane Damage Caused by DMSO**

To verify the damaging effect of different concentrations of DMSO and the effect of different working time at a specific concentration of DMSO on the plasma membrane, dynamic morphological change of plasma membrane caused by DMSO was tracked using CSP-DBO dye. A piece of onion inner epidermis from fresh onion was first stained with CSP-DBO (10.0  $\mu\text{M}$ ) for 2 minutes, and then the stained onion epidermal cells were placed in different concentrations of DMSO solution for several seconds to damage the plasma membrane. Then the onion inner epidermis was placed on the slide glass for imaging experiments. By comparing the confocal images of cells treated with different concentrations of DMSO, critical concentration of DMSO in aqueous solution which can cause significant damage to plasma membrane can be determined. To investigate the change of plasma membrane caused by DMSO at the critical concentration with incubation time, four piece of onion inner epidermis stained with CSP-DBO (10.0  $\mu\text{M}$ ) first were treated with 9% aqueous DMSO solution for different incubation time of 0, 10, 20 and 30 min respectively. After DMSO treatment, the four groups of onion inner epidermis were placed on slides and imaged using a Zeiss model LSM 880 confocal laser scanning microscope (Germany) with excitation at 561 nm respectively.

#### **1.15 Three-Dimensional Imaging of Plasma Membrane of Onion Epidermal Cells**

Three-dimensional imaging of onion epidermal cells was performed as follows. A piece of onion internal epidermis from fresh onion was incubated in 2 mL of MS culture containing 10.0  $\mu\text{M}$  CSP-DBO for 2 min, and then the epidermis was placed on the slide glass. Confocal images of onion epidermal

cells were collected every 1  $\mu\text{m}$  from the top to the bottom under the optimal conditions. The three-dimensional images were obtained using the ImageJ software based on all the 2D confocal images. The same protocol was applied to obtain 3D images of plasma membrane after plasmolysis, where the stain solution was replaced with a NaCl solution (0.3 g/mL) containing CSP-DBO.

### 1.16 The Statistical Data Process Details of Quantitative Analysis

The data statistics quantified including signal to noise ratio ( $f_{\text{Signal}}/f_{\text{Background}}$ ) of stained plasma membrane, signal ratios of plasma membrane to cell wall ( $S_{\text{Membrane}}/S_{\text{Wall}}$ ), and signal ratio of imaging signal ( $S_{\text{Signal}}$ ) were presented by the software "ImageJ" and "Adobe Photoshop CS6". We used " $f_{\text{Signal}}/f_{\text{Background}}$ " to represent the brightness by "ImageJ". Import the merged images into the software and separated the channels, selected the dark field channel and clicked "Threshold" to calculate the Mean (average gray value). For the signal-to-noise ratio of the membrane and the wall ( $S_{\text{Membrane}}/S_{\text{Wall}}$ ): select the box tool to select the cell membrane and the cell wall to obtain the mean gray value to calculate the ratio. Signal ratio (" $S_{\text{Signal}}$ ") from high-resolution pixel analysis was realized by "Adobe Photoshop CS6" software. Import the image and use the "Color Picker" in the "Color Range" option to select the "signal region" with red. After finishing the selection, the "Measurement Log" operation can be performed, and the obtained "Area" corresponds to the " $S_{\text{Signal}}$ ". Repeating the same operation, the area of "non-signal region" can be gained by reverse selection.

## 2. Synthesis and Characterization of Dyes

**Synthesis of N,N-dihexylaniline (1).** 1-Bromohexane (16.51 g, 100 mmol) was added to a solution of aniline (2.80 g, 30 mmol),  $\text{K}_2\text{CO}_3$  (16.50 g, 120 mmol) and KI (6.64 g, 40 mmol) in DMF (50 mL). After refluxing for 12 h, the reaction mixture was poured into  $\text{H}_2\text{O}$  (100 mL) and extracted with  $\text{CH}_2\text{Cl}_2$  (3 $\times$ 50 mL). The organic phase was dried over anhydrous  $\text{Na}_2\text{SO}_4$ , and the

crude product was purified by column chromatography (pure petroleum ether) on silica gel. The solvent was removed to give compound 1 as a faint yellow liquid (6.68 g, 85%). Molecular formula: C<sub>18</sub>H<sub>31</sub>N. <sup>1</sup>H NMR (600 MHz, CDCl<sub>3</sub>) δ (ppm): 7.26 – 7.23 (m, 2H), 6.69 – 6.65 (m, 3H), 3.29 (t, *J* = 6.0 Hz, 4H), 1.63 – 1.59 (m, 4H), 1.37 – 1.34 (m, 12H), 0.95 (t, *J* = 6.0 Hz, 6H). <sup>13</sup>C NMR (151 MHz, CDCl<sub>3</sub>) δ (ppm): 148.18, 129.20, 115.03, 111.65, 51.08, 31.80, 27.23, 26.92, 22.75, 14.10. ESI HRMS (*m/z*): calcd. for C<sub>18</sub>H<sub>31</sub>N [M+H]<sup>+</sup> 262.2535, found 262.2550.

**Synthesis of 4-(dihexylamino)benzaldehyde (2).** N,N-dihexylaniline (2.00 g, 7.65 mmol) was added into a 100 mL round-bottom flask containing 50 mL DMF in ice bath. Then phosphorus oxychloride (2.02 g, 13.23 mmol) was slowly dropped into the aforementioned solution with vigorous stirring. The reaction mixture was stirred and heated for 4 h at 100 °C, and then 100 mL ice water was added into the mixture slowly after cooling to room temperature. Na<sub>2</sub>CO<sub>3</sub> was used to adjust the pH of the solution under vigorous stirring. After the pH in the solution reached 7.0, the solution was extracted with CH<sub>2</sub>Cl<sub>2</sub> (3×50 mL). The organic phase was dried over anhydrous Na<sub>2</sub>SO<sub>4</sub>, and then the crude was purified by column chromatography (petroleum/CH<sub>2</sub>Cl<sub>2</sub> (3:1 v/v)) on silica gel. The solvent was removed to give compound 2 as a yellow liquid (1.16 g, 80%). Molecular formula: C<sub>19</sub>H<sub>31</sub>NO. <sup>1</sup>H NMR (600 MHz, CDCl<sub>3</sub>) δ (ppm): 9.69 (s, 1H), 7.69 (d, *J* = 8.7 Hz, 2H), 6.63 (d, *J* = 9.0 Hz, 2H), 3.33 (t, *J* = 6.0 Hz, 4H), 1.63 - 1.58 (m, 4H), 1.35 – 1.31 (m, 12H), 0.91 – 0.89 (t, *J* = 6.0 Hz, 6H). <sup>13</sup>C NMR (151 MHz, CDCl<sub>3</sub>) δ (ppm): 189.96, 152.60, 132.23, 124.47, 110.65, 51.13, 31.65, 27.12, 26.73, 22.66, 14.04. ESI HRMS (*m/z*): calcd. for C<sub>19</sub>H<sub>31</sub>NO [M+H]<sup>+</sup> 290.2484, found 290.2474.

**Synthesis of (Z)-3-(4-(dihexylamino)phenyl)-2-(pyridin-4-yl)acrylonitrile (3).** 4-(Dihexylamino)benzaldehyde (2.0 g, 6.91 mmol) was dissolved in methanol and stirred at room temperature. To this solution, 4-pyridine acetonitrile (0.98 g, 8.29 mmol) and sodium methoxide (0.63 g, 11.75 mmol)

were added, and then the reaction mixture was stirred at 80 °C for 5 h. After cooling to room temperature, the mixture was extracted with ethyl acetate. The organic layer was washed with water 3 times (3×50 mL) and dried by anhydrous Na<sub>2</sub>SO<sub>4</sub>. All solvents were removed by rotary evaporation. The crude product was purified by column chromatography (EA:PE=2:1) to give a brownish and gelatinous product (2.42 g, 90%). Molecular formula: C<sub>26</sub>H<sub>35</sub>N<sub>3</sub>. <sup>1</sup>H NMR (600 MHz, CDCl<sub>3</sub>), δ (ppm): 8.61 (d, *J* = 5.6 Hz, 2H), 7.88 (d, *J* = 9.0 Hz, 2H), 7.55 (s, 1H), 7.51 (d, *J* = 6.2 Hz, 2H), 6.66 (d, *J* = 9.1 Hz, 2H), 3.34 (t, *J* = 6.0 Hz, 4H), 1.63 – 1.59 (m, *J* = 12.0 Hz, 4H), 1.35 – 1.32 (m, *J* = 12.0 Hz, 12H), 0.92 – 0.90 (m, *J* = 6.0 Hz, 6H). <sup>13</sup>C NMR (101 MHz, CDCl<sub>3</sub>), δ (ppm): 150.66, 150.17, 144.87, 143.33, 132.56, 119.80, 119.24, 118.75, 111.26, 100.02, 77.36, 77.04, 76.73, 51.11, 31.67, 27.25, 26.76, 22.69, 14.07. ESI HRMS (*m/z*): calcd. for C<sub>26</sub>H<sub>35</sub>N<sub>3</sub> [M+H]<sup>+</sup>: 390.2909, found: 390.2902.

**Synthesis of (Z)-4-(1-cyano-2-(4-(dihexylamino)phenyl)vinyl)-1-methylpyridin-1-ium iodide (CSP).** A certain amount of (Z)-3-(4-(dihexylamino)phenyl)-2-(pyridin-4-yl)acrylonitrile (1.5 g, 3.85 mmol) was dissolved in acetonitrile at room temperature. To this solution, iodomethane (5.46 g, 38.5 mmol) was added, and then the reaction mixture was stirred at 80 °C for 5 h. After cooling to room temperature, the solvent was removed by rotary evaporation. The crude product was washed with a mixed solution of petroleum ether and acetone (petroleum ether: ethyl alcohol =50:1) at least three times. The residual solvent was evaporated under reduced pressure to give a dark red solid (1.74 g, 85%). Molecular formula: C<sub>27</sub>H<sub>38</sub>N<sub>3</sub>I. <sup>1</sup>H NMR (400 MHz, CDCl<sub>3</sub>), δ (ppm): 8.72 (d, *J* = 7.0 Hz, 2H), 8.14 (s, 1H), 8.10 (d, *J* = 7.2 Hz, 2H), 8.04 (d, *J* = 9.1 Hz, 2H), 6.56 (d, *J* = 9.3 Hz, 2H), 4.37 (s, 3H), 3.27 (t, *J* = 8.0 Hz, 4H), 1.56 -1.48 (m, 4H), 1.26 -1.21 (m, 12H), 0.80 (t, *J* = 8.0 Hz, 6H). <sup>13</sup>C NMR (101 MHz, CDCl<sub>3</sub>), δ (ppm): 152.96, 152.27, 150.73, 144.04, 135.73, 121.46, 119.96,

117.91, 111.97, 93.99, 77.37, 77.05, 76.74, 51.45, 48.06, 31.58, 27.39, 26.69, 22.63, 14.02. ESI HRMS (m/z): calcd. for  $C_{27}H_{38}N_3I$   $[M-I]^+$  404.3061, found: 404.3058.

**Synthesis of (Z)-4-(1-cyano-2-(4-(dihexylamino)phenyl)vinyl)-1-(3-(triethylammonio)propyl)pyridin-1-ium bromide (CSP-TEA).** A certain amount of 3-bromo-N,N,N-triethylpropan-1-aminium (0.65 g, 2.14 mmol) was added to an acetonitrile solution containing (Z)-3-(4-(dihexylamino)phenyl)-2-(pyridin-4-yl)acrylonitrile (1.0 g, 2.57 mmol), and the reaction mixture was refluxed for 20 h. After cooling to room temperature, the solvent was removed by rotary evaporation. The crude product was washed with a mixed solution of petroleum ether and acetone (petroleum ether: ethyl alcohol =50:1) at least three times. The residual solvent was evaporated under reduced pressure to give a dark red solid (1.26 g, 85%). Molecular formula:  $C_{35}H_{56}Br_2N_4$ .  $^1H$  NMR (600 MHz,  $CDCl_3$ ),  $\delta$  (ppm): 9.57 (s, 2H), 8.16 – 8.05 (m, 5H), 6.63 (d,  $J = 8.2$  Hz, 2H), 3.75 (s, 2H), 3.47 -3.43 (m,  $J = 7.5$  Hz, 6H), 3.34 (t,  $J = 7.9$  Hz, 4H), 2.96 (s, 2H), 2.77 (s, 2H), 1.59 (s, 4H), 1.41 (t,  $J = 7.2$  Hz, 9H), 1.30 (s, 12H), 0.88 (t,  $J = 6.1$  Hz, 6H).  $^{13}C$  NMR (151 MHz,  $CDCl_3$ ),  $\delta$  (ppm): 152.78, 152.31, 150.53, 144.44, 135.40, 121.35, 119.88, 111.89, 94.47, 77.29, 77.08, 76.87, 55.98, 54.21, 53.95, 51.39, 31.56, 27.36, 26.67, 25.18, 22.62, 14.02, 8.41, 8.27. ESI HRMS (m/z): calcd. for  $C_{35}H_{56}Br_2N_4$ .  $[M-2Br]^{2+}$ : 266.2247, found: 266.2249.

**Synthesis of (Z)-4-(1-cyano-2-(4-(dihexylamino)phenyl)vinyl)-1-(3-(triphenylphosphonio)propyl)pyridin-1-ium bromide (CSP-TPP).** A certain amount of 3-bromopropyl)triphenylphosphonium (0.6 g, 1.28 mmol) was added to an acetonitrile solution containing (Z)-3-(4-(dihexylamino)phenyl)-2-(pyridin-4-yl)acrylonitrile (1.0 g, 2.57 mmol), and the reaction mixture was refluxed for 20 h. After cooling to room temperature, the solvent was removed by rotary evaporation. The crude product was washed with a mixed solution of petroleum ether and acetone (petroleum ether: ethyl alcohol =50:1) at least



three times. The residual solvent was evaporated under reduced pressure to give a dark red solid (0.84 g, 77%). Molecular formula:  $C_{47}H_{56}Br_2N_3P$ .  $^1H$  NMR (600 MHz,  $CDCl_3$ ),  $\delta$  (ppm): 9.75 (d,  $J = 6.4$  Hz, 2H), 8.02 (d,  $J = 8.6$  Hz, 2H), 7.98 (d,  $J = 6.9$  Hz, 3H), 7.88 – 7.85 (m, 6H), 7.78 – 7.74 (m, 3H), 7.70 – 7.67 (m, 6H), 6.64 (d,  $J = 9.0$  Hz, 2H), 5.39 (t,  $J = 6.0$  Hz, 2H), 3.91 - 3.84 (m, 2H), 3.36 (t,  $J = 6.0$  Hz, 4H), 2.54 – 2.50 (m, 2H), 2.15 (s, 4H), 1.33 – 1.28 (m, 12H), 0.87 (t,  $J = 6.0$  Hz, 6H).  $^{13}C$  NMR (151 MHz,  $CD_3OD$ ),  $\delta$  (ppm): 153.12, 152.85, 150.62, 143.56, 135.09, 133.70, 133.49, 130.34, 121.20, 119.83, 118.11, 117.53, 111.78, 94.07, 58.87, 50.78, 31.42, 27.09, 26.27, 24.14, 22.32, 19.18, 13.00. ESI HRMS ( $m/z$ ): calcd. for  $C_{47}H_{56}Br_2N_3P$ .  $[M-2Br]^{2+}$ : 346.7101, found: 346.7108.

**Synthesis of (Z)-1-(3-(4-(1-cyano-2-(4-(dihexylamino)phenyl)vinyl)pyridin-1-ium-1-yl)propyl)-1,4-diazabicyclo[2.2.2]octan-1-ium bromide (CSP-DBO).** A certain amount of 1-(3-bromopropyl)-1,4-diazabicyclo[2.2.2]octan-1-ium (0.67 g, 2.14 mmol) was added to an acetonitrile solution containing (Z)-3-(4-(dihexylamino)phenyl)-2-(pyridin-4-yl)acrylonitrile (1.0 g, 2.57 mmol), and the reaction mixture was refluxed for 20 h. After cooling to room temperature, the solvent was removed by rotary evaporation. The crude product was washed with a mixed solution of petroleum ether and acetone (petroleum ether: ethyl alcohol =50:1) at least three times. The residual solvent was evaporated under reduced pressure to give a dark red solid (1.08 g, 72%). Molecular formula:  $C_{35}H_{53}Br_2N_5$ .  $^1H$  NMR (600 MHz,  $CD_3OD$ ),  $\delta$  (ppm): 8.84 (d,  $J = 7.2$  Hz, 2H), 8.32 (s, 1H), 8.21 (d,  $J = 7.3$  Hz, 2H), 8.12 (d,  $J = 9.0$  Hz, 2H), 6.86 (d,  $J = 9.3$  Hz, 2H), 4.63 (t,  $J = 7.7$  Hz, 2H), 4.30 – 4.23 (m, 4H), 3.52 – 3.47 (m, 8H), 3.26 - 3.22 (m, 6H), 2.60 – 2.55 (m, 2H), 1.69 - 1.64 (m, 4H), 1.42 - 1.34 (m, 12H), 0.94 – 0.92 (t,  $J = 6.0$  Hz, 6H).  $^{13}C$  NMR (151 MHz,  $CD_3OD$ ),  $\delta$  (ppm): 153.23, 150.71, 143.54, 134.96, 121.16, 119.83, 117.49, 111.82, 94.01, 60.33, 56.40, 52.46, 51.50,

50.76, 44.64, 31.41, 27.06, 26.25, 23.67, 22.30, 12.96. ESI HRMS (m/z): calcd. for  $C_{35}H_{53}Br_2N_5$ .  $[M-2Br]^{2+}$ : 271.7145, found: 271.7155.

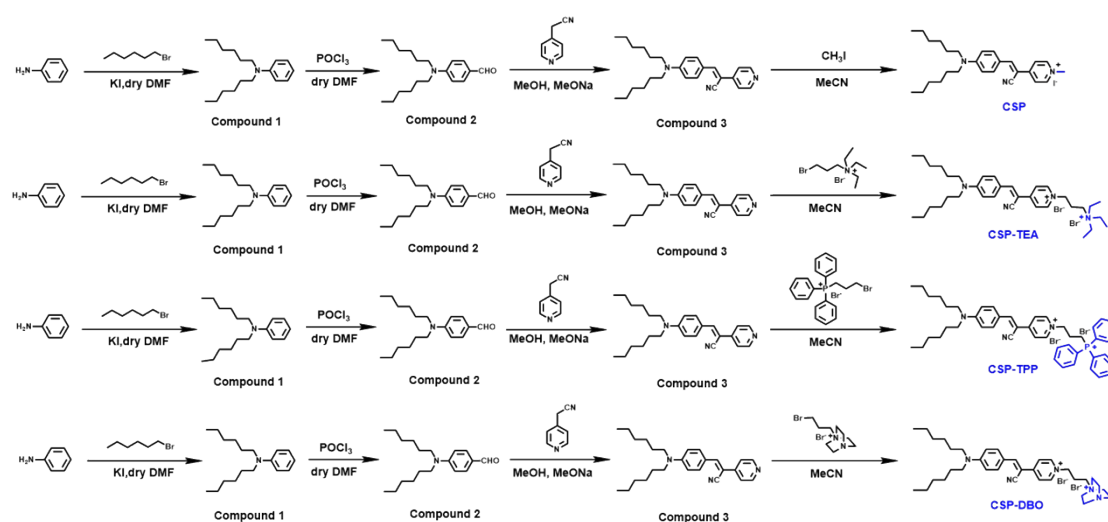
**Synthesis of 3-bromo-N,N,N-triethylpropan-1-ammonium bromide.** 1,3-Dibromopropane (4.04 g, 20 mmol) was added to a solution of triethylamine (1.01 g, 10 mmol) in 50 mL acetone, and then the mixture was refluxed for 8 hours. After the reaction was completed, white crystals precipitated on the wall of the round bottom flask. The precipitates were filtered out and washed with acetone. The final product was dried to give final product as a white powder (2.79 g, 92%). Molecular formula:  $C_9H_{21}Br_2N$ .  $^1H$  NMR (400 MHz,  $D_2O$ ),  $\delta$  (ppm): 3.51 (t,  $J = 4.0$ , 2H), 3.33 – 3.25 (m, 8H), 2.28 – 2.21 (m, 2H), 1.25 (t,  $J = 7.3$  Hz, 9H).  $^{13}C$  NMR (151 MHz,  $D_2O$ ),  $\delta$  (ppm): 55.25, 53.09, 52.75, 29.17, 24.14, 6.60. ESI HRMS (m/z): calcd. for  $C_9H_{21}Br_2N$ .  $[M-Br]^+$  222.0850, found 222.0852.

**Synthesis of (3-bromopropyl)triphenylphosphonium bromide.** 1,3-Dibromopropane (2.02 g 10 mmol) was added to a solution of triphenylphosphine (2.62 g, 10 mmol) in 30 mL toluene under  $N_2$  atmosphere. White crystals precipitated on the wall of the round bottom flask after the solution was stirred at room temperature for 20 h. The precipitates were filtered out and washed with dichloromethane. The final product was dried with a rotary evaporator to give a white powder (3.90 g, 84%). Molecular formula:  $C_{21}H_{21}Br_2P$ .  $^1H$  NMR (600 MHz,  $CD_3OD$ ),  $\delta$  (ppm): 7.94 – 7.91 (m, 3H), 7.86 – 7.82 (m, 6H), 7.80 – 7.77 (m, 6H), 3.66 – 3.58 (m, 4H), 2.25 – 2.19 (m, 2H).  $^{13}C$  NMR (151 MHz,  $CD_3OD$ ),  $\delta$  (ppm): 135.09, 133.49, 133.49, 130.28, 118.40, 117.83, 31.76, 25.73, 20.55. ESI HRMS (m/z): calcd. for  $C_{21}H_{21}Br_2P$ .  $[M-Br]^+$ : 383.0559, found: 383.0555.

**Synthesis of 1-(3-bromopropyl)-1,4-diazabicyclo[2.2.2]octan-1-ium bromide.** 1,3-Dibromopropane (2.02 g 10 mmol) was added to a solution of 1,4-diazabicyclo[2.2.2]octane (1.12 g, 10 mmol) in 100 mL acetone. White crystals precipitated on the wall of the round bottom flask after the solution

was stirred at room temperature for 3 hours. The precipitates were filtered out and washed with acetone. The final product was dried with a rotary evaporator to give a white powder (2.64 g, 84%). Molecular formula:  $C_9H_{18}Br_2N_2$ .  $^1H$  NMR (600 MHz,  $D_2O$ ),  $\delta$  (ppm): 3.54 (t,  $J = 6.1$  Hz, 2H), 3.47 (d,  $J = 8.2$  Hz, 2H), 3.44 (t,  $J = 6.0$  Hz, 2H), 3.21 (t,  $J = 6.0$  Hz, 6H), 2.40 – 2.36 (m, 2H).  $^{13}C$  NMR (151 MHz,  $D_2O$ ) 63.11, 52.31, 44.17, 29.07, 24.38. ESI HRMS ( $m/z$ ): calcd. for  $C_9H_{18}Br_2N_2$ .  $[M-Br]^+$ : 233.0648, found: 233.0647.

### 3. Supplementary Schemes and Figures



**Scheme S1.** Synthesis routes of CSP, CSP-TEA, CSP-TPP and CSP-DBO.

Compounds	$\lambda_{ex}$ (nm)	$\lambda_{em}$ (nm)
CSP	561	590-650
CSP-TPP	561	590-657
CSP-TEA	561	590-650
CSP-DBO	561	590-650

**Table S1.** The optical parameters of the dyes used for confocal imaging experiments.

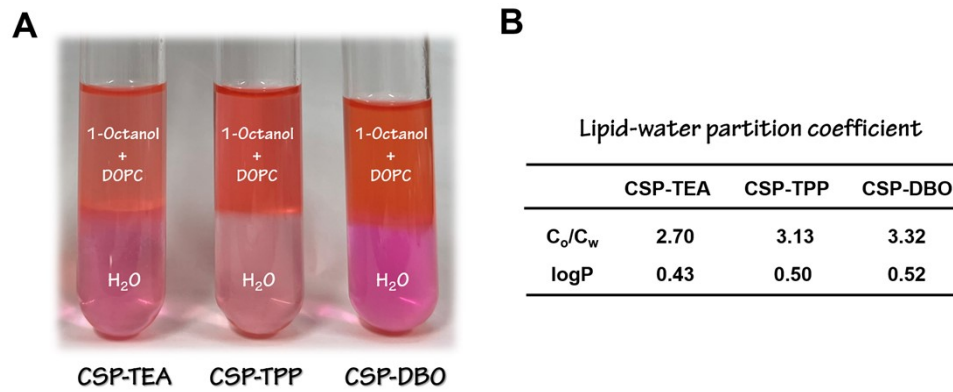


**Figure S1.** (A) Qualitative illustration of the distribution of CSP-TEA, CSP-TPP and CSP-DBO between 1-Octanol containing DOPC (40  $\mu$ M) and water. (B) Quantitative lipid-water partition coefficient (logP) of CSP-TEA, CSP-TPP and CSP-DBO.

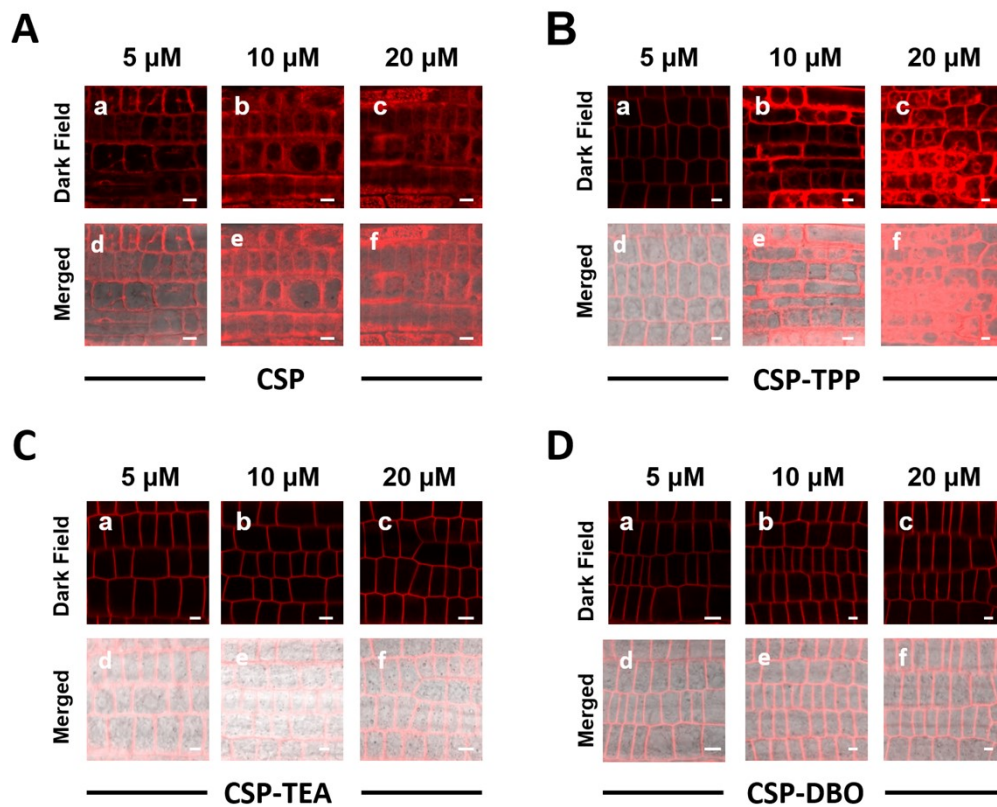


**Figure S2.** Laser scanning confocal microscopy images of *Arabidopsis thaliana* stained with different amounts of dyes at different staining time. (A) CSP for 2 min: (a, d) 5.0  $\mu$ M; (b, e) 10.0  $\mu$ M; (c, f) 20.0  $\mu$ M; Scale bar = 50  $\mu$ m. (B) CSP-TPP for 2 min: (a, d) 5.0  $\mu$ M; (b, e) 10.0  $\mu$ M; (c, f) 20.0  $\mu$ M; Scale bar= 5  $\mu$ m (a, d, c, f), Scale bar= 10  $\mu$ m (b, e). (C) CSP-TEA for 2 min: (a, d) 5.0  $\mu$ M; (b, e) 10.0  $\mu$ M; (c, f) 20.0  $\mu$ M; Scale bar= 5  $\mu$ m (a, d), Scale bar= 10  $\mu$ m (b, e, c, f). (D) CSP-DBO for 2 min: (a, d) 5.0  $\mu$ M; (b, e) 10.0  $\mu$ M; (c, f) 20.0  $\mu$ M; Scale bar= 10  $\mu$ m (a, d), Scale bar= 5  $\mu$ m (b, e, c, f).

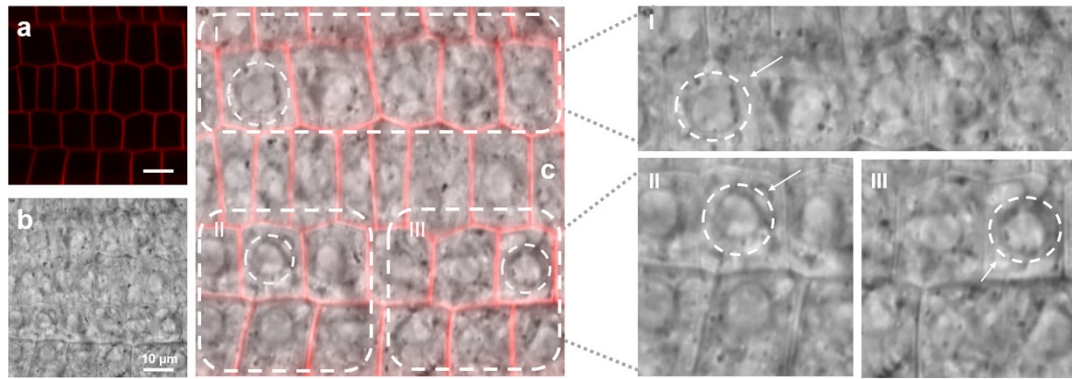


**Figure S3.** Laser scanning confocal microscopy images in seedling roots tip cells of *Arabidopsis thaliana* stained with CSP-DBO (10.0  $\mu\text{M}$  probes incubated for 2 min). (a) The plasma membrane was labelled with red color in dark field; (b) the vacuoles were observed at the center of the cells in bright field; (c) in the merged image, no overlap between the plasma membrane and the vacuole was observed. Scale bar = 10  $\mu\text{m}$ .

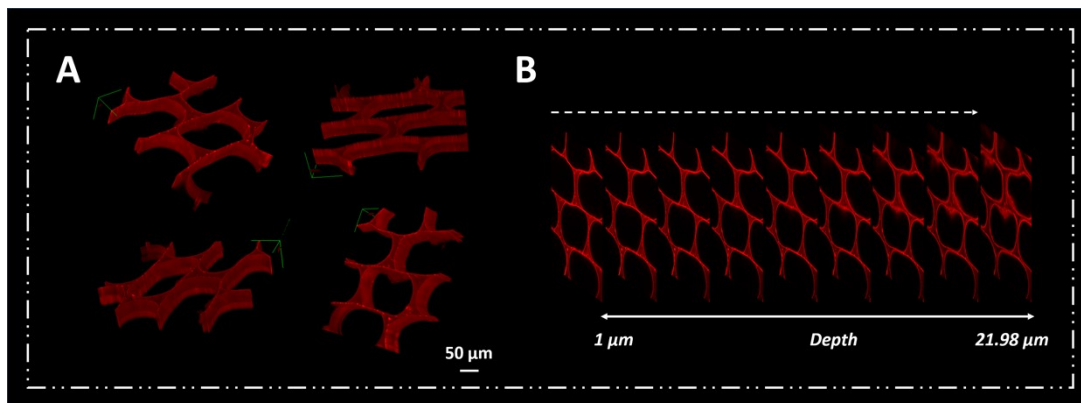


**Figure S4.** (A) 3D tracking of morphological changes of the plasma membrane in onion epidermal cells stained with CSP-DBO (20  $\mu\text{M}$ ) during water loss process. Scale bar = 50  $\mu\text{m}$ . (B) Z-stack images of onion epidermal cells from 1 to 21.98  $\mu\text{m}$  after staining with CSP-DBO (20  $\mu\text{M}$ ).

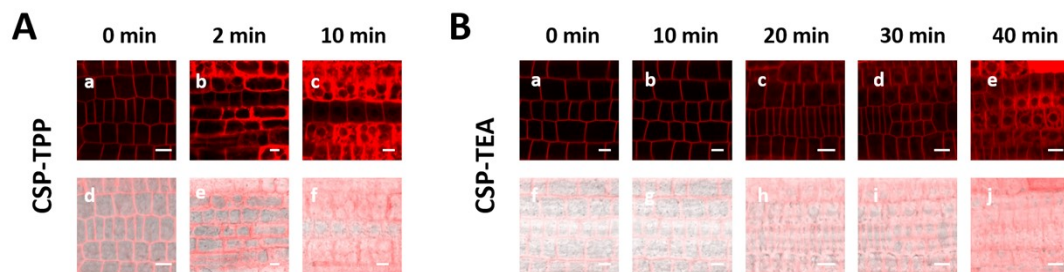


**Figure S5.** Laser scanning confocal microscopy images in seedling roots of *Arabidopsis thaliana* stained with (A) CSP-TPP (5.0  $\mu\text{M}$  probes incubated for 2 min) (B) CSP-TEA (10.0  $\mu\text{M}$  probes incubated for 2 min) at various time points. Scale bar = 10  $\mu\text{m}$ .

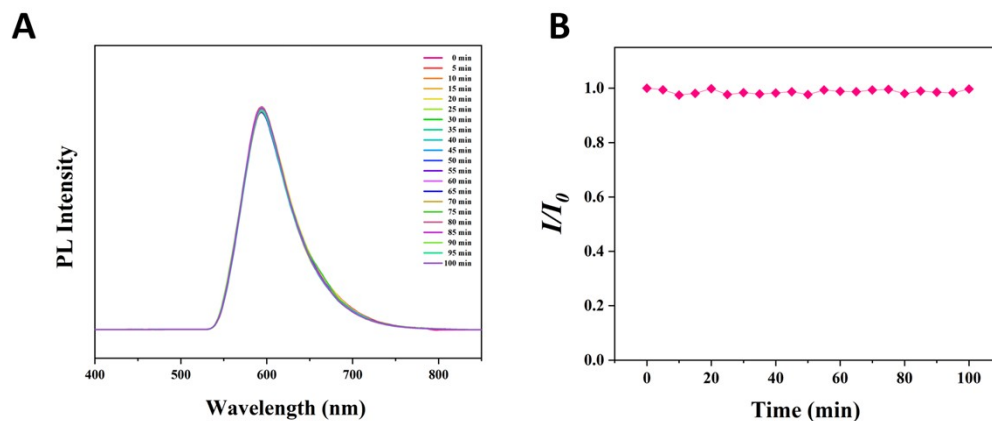


**Figure S6.** (A) UV-visible spectrum of CSP-DBO (10.0  $\mu\text{M}$ ) in  $\text{H}_2\text{O}$  at various time points via a long-term irradiation (561 nm 20 mW); (B) The change in absorbance of the peak at 513 nm of CSP-DBO (10.0  $\mu\text{M}$ ) in  $\text{H}_2\text{O}$  versus irradiation time by using the excitation source of 561 nm 20 mW.

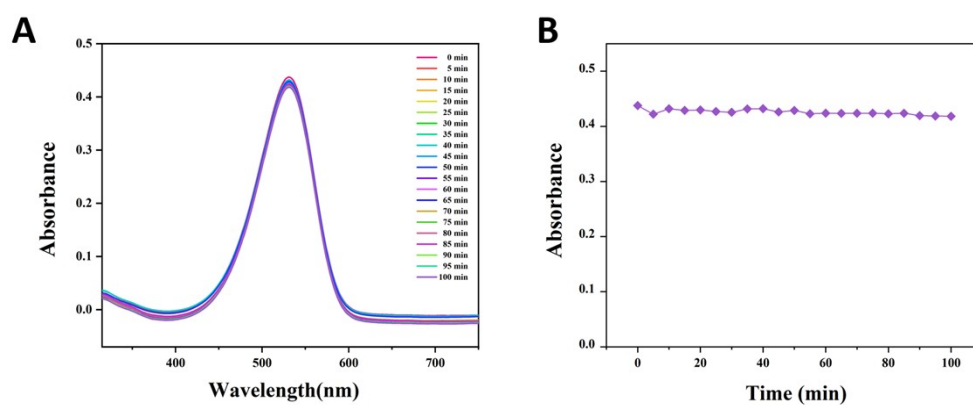


**Figure S7.** (A) PL spectra of CSP-DBO (10.0  $\mu\text{M}$ ) in  $\text{H}_2\text{O}$  at various time points via a long-term irradiation (561 nm 20 mW); (B) The change of PL spectra of CSP-DBO (10.0  $\mu\text{M}$ ) in  $\text{H}_2\text{O}$  at various time points via a long-term irradiation (561 nm 20 mW).

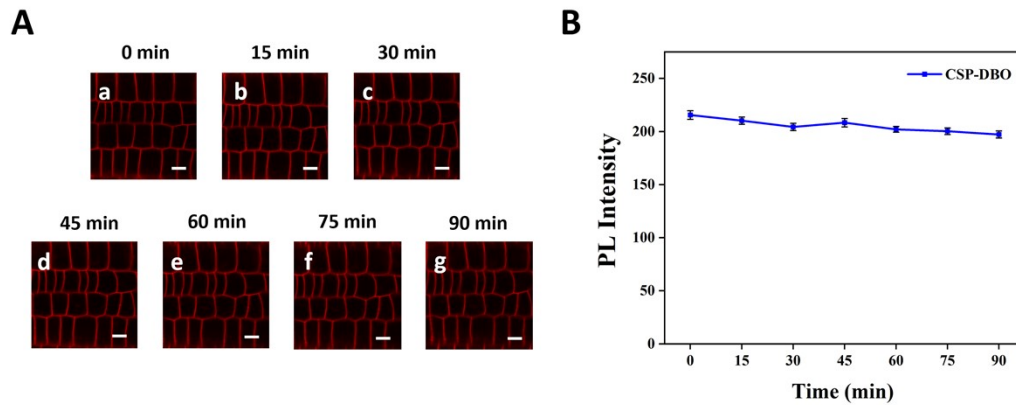


**Figure S8.** (A) The changes of laser scanning confocal microscopy images in seedling roots of *Arabidopsis thaliana* stained with CSP-DBO (10.0  $\mu\text{M}$ ) for 2 min versus irradiation time at 561 nm using the excitation source of the used microscope: (a) CSP-DBO (0 min); (b) CSP-DBO (15 min); (c) CSP-DBO (30 min); (d) CSP-DBO (45 min); (e) CSP-DBO (60 min); (f) CSP-DBO (75 min); (g) CSP-DBO (90 min). Scale bar = 10  $\mu\text{m}$ . (B) The change of PL intensity of CSP-DBO inserted inside the cell membranes versus irradiation time at 561 nm using the excitation source of the used microscope.

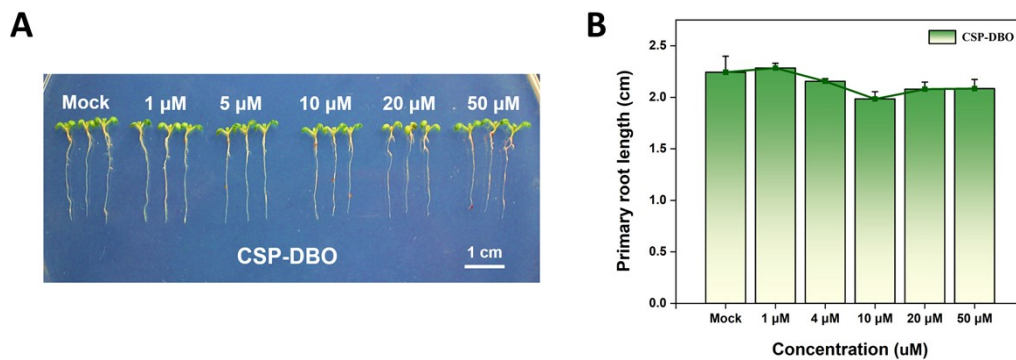


**Figure S9.** (A) Photographs of representative *Arabidopsis thaliana* seedlings incubated without (Mock) and with different concentrations of CSP-DBO (1.0  $\mu\text{M}$  to 50.0  $\mu\text{M}$ ) after 6 days. (b) Average root lengths of *Arabidopsis thaliana* seedlings incubated without (Mock) and with different concentrations of CSP-DBO (1.0  $\mu\text{M}$  to 50.0  $\mu\text{M}$ ) after 6 days.

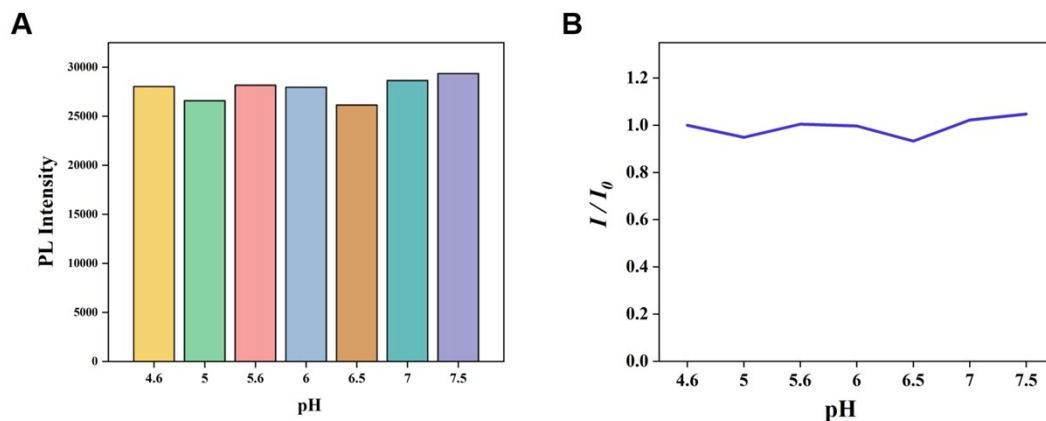


**Figure S10.** (A) Change in PL intensity of the CSP-DBO in PBS (20.0  $\mu\text{M}$ ) versus pH values.  $\lambda_{\text{em}} = 515 \text{ nm}$ ; (B) Change in mean PL intensity of the CSP-DBO in PBS (20.0  $\mu\text{M}$ ) versus pH values by using line charts.  $\lambda_{\text{em}} = 515 \text{ nm}$ .

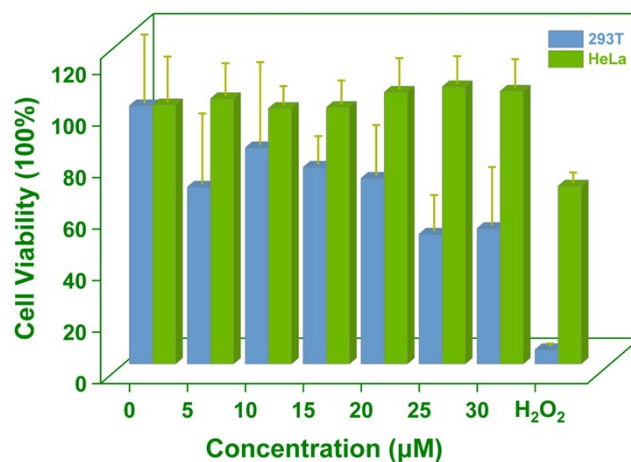


**Figure S11.** Viability of cancer cell (HeLa) and normal cell (HEK293T) incubated with different concentrations of CSP-DBO (0  $\mu\text{M}$  to 30.0  $\mu\text{M}$ ) and 1 mM  $\text{H}_2\text{O}_2$  (positive control) after 24 h.

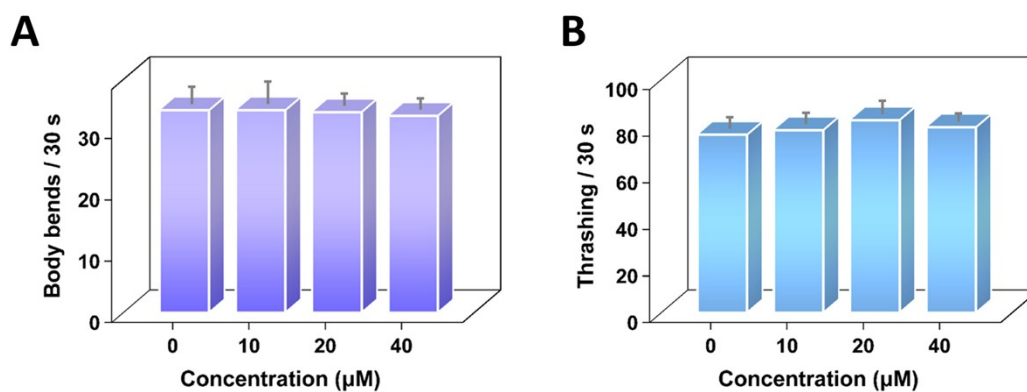


**Figure S12.** Evaluation of biocompatibility of CSP-DBO in *C. elegans*. (A) The frequency of body bends within 30s; (B) The frequency of head thrashes within 30s.



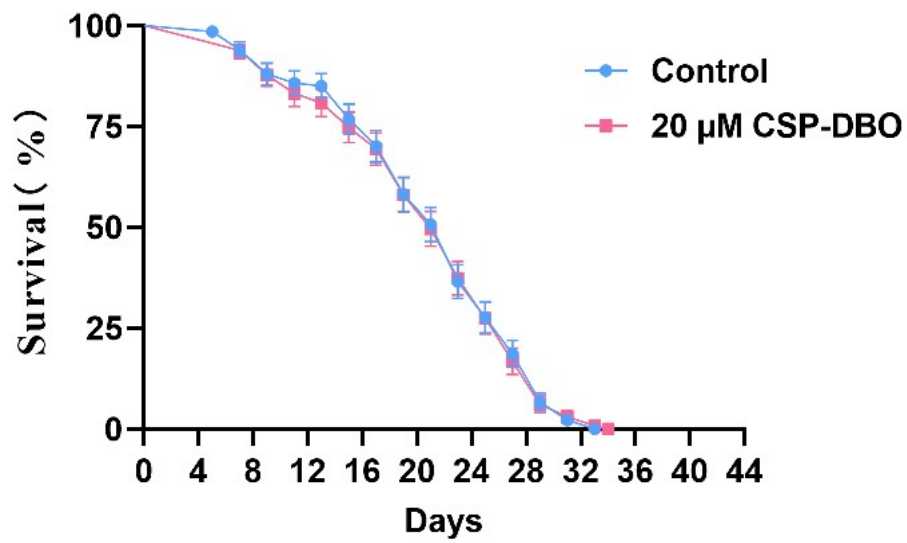
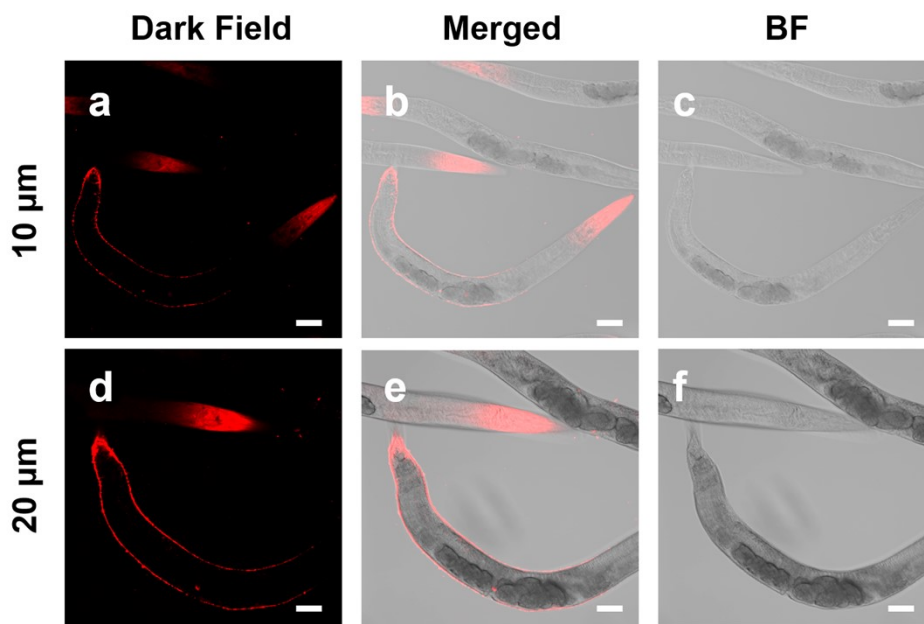


**Figure S13.** Evaluation the biocompatibility (lifespan) of CSP-DBO in *C. elegans*.



*C. elegans* stained by CSP-DBO

**Figure S14.** Laser scanning confocal microscopy images of *C. elegans* stained with CSP-DBO (a – c: 10.0 μM, 30min; d – f: 20.0 μM, 30min). Scale bar = 50 μm.

#### 4. Spectra of Compounds

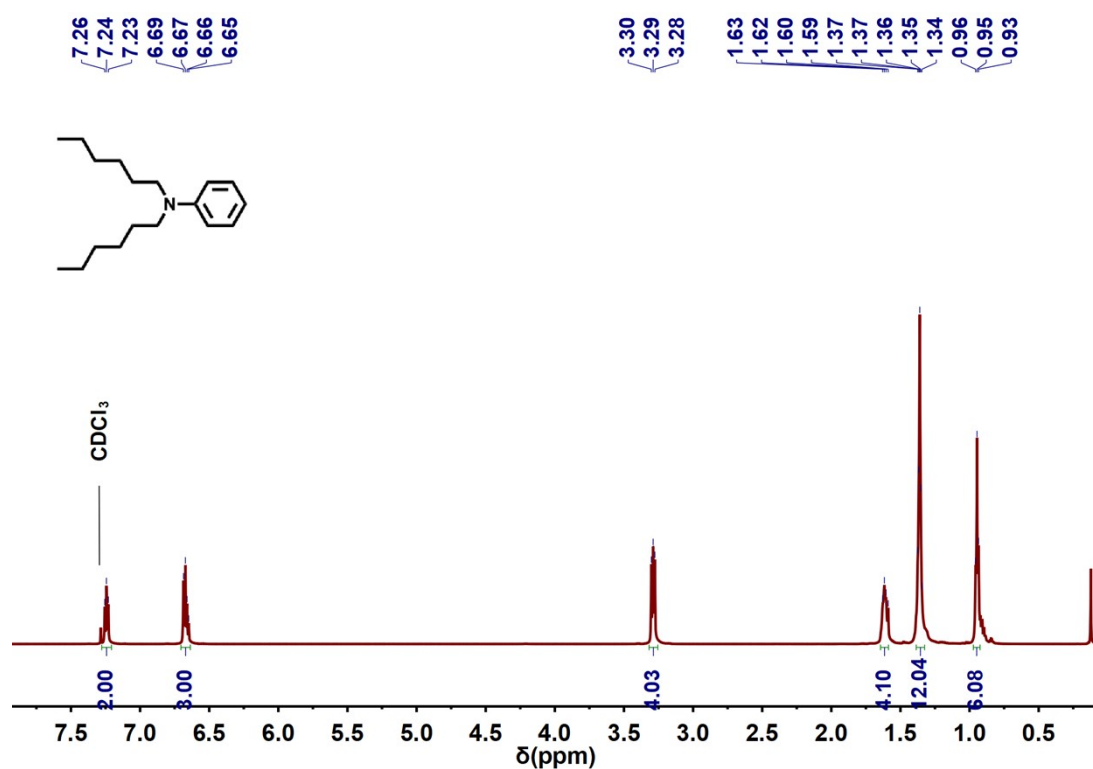


Figure S15.  $^1\text{H}$  NMR spectra of N,N-dihexylaniline (1) in  $\text{CDCl}_3$

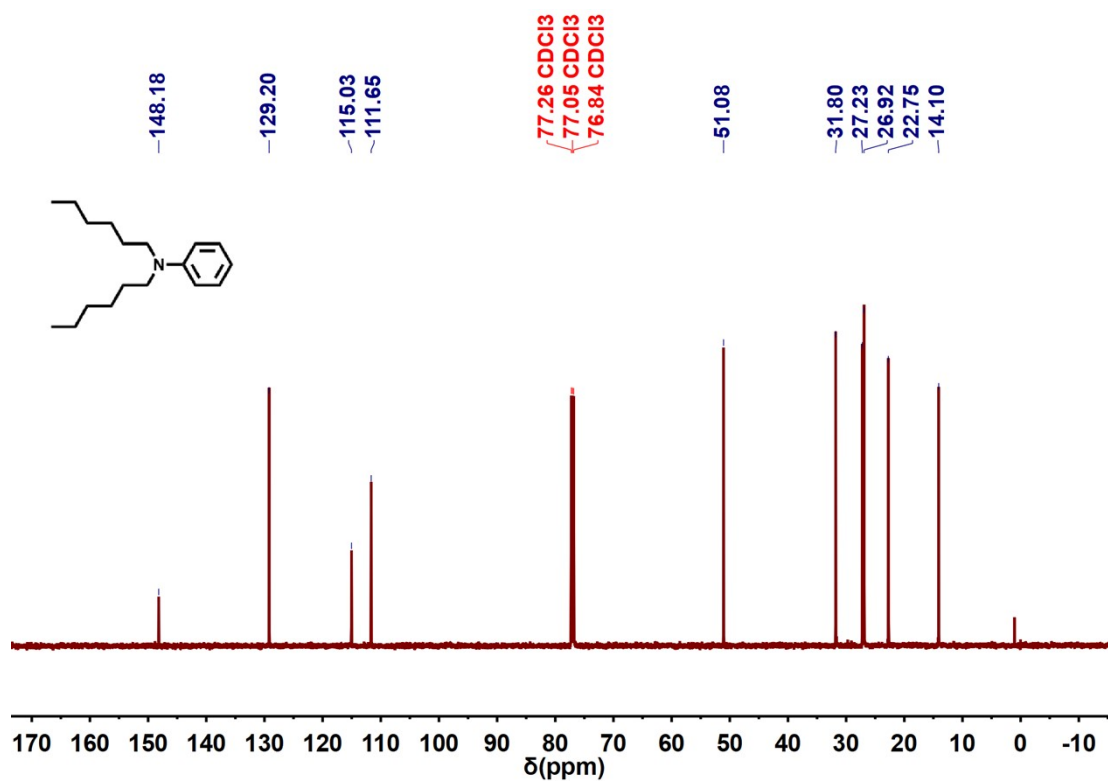


Figure S16.  $^{13}\text{C}$  NMR spectra of N,N-dihexylaniline (1) in  $\text{CDCl}_3$

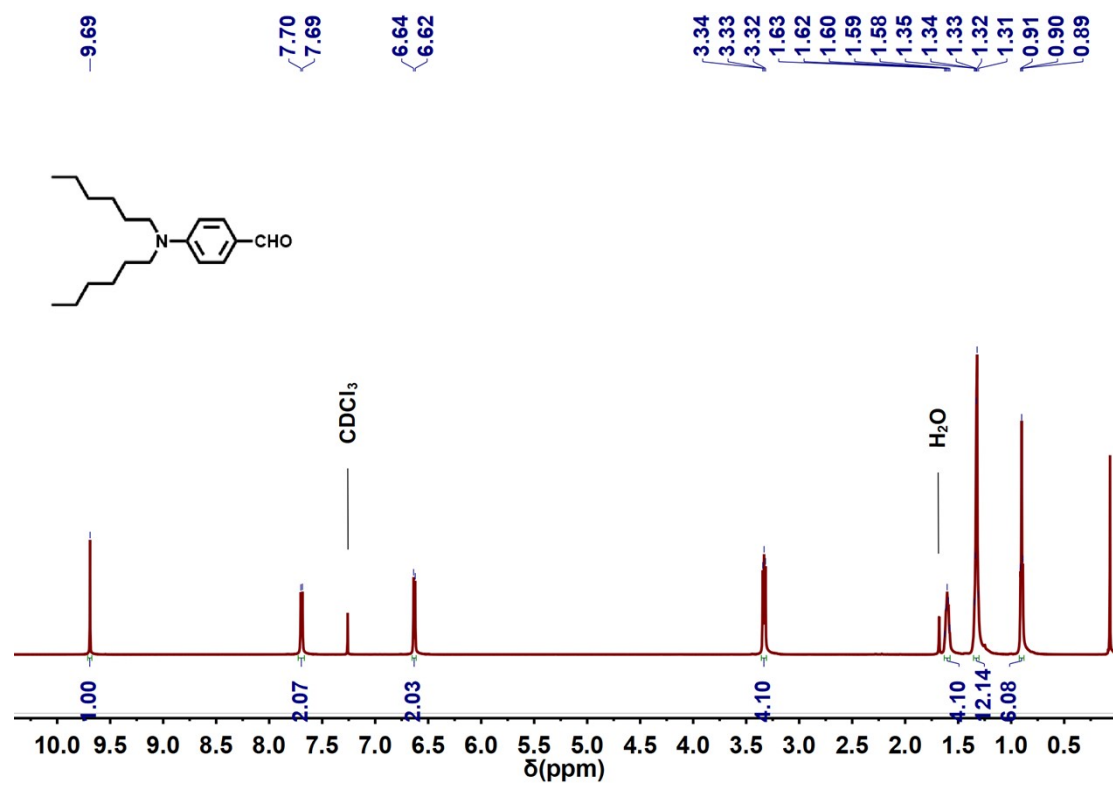


Figure S17. <sup>1</sup>H NMR spectra of 4-(dihexylamino)benzaldehyde (2) in CDCl<sub>3</sub>

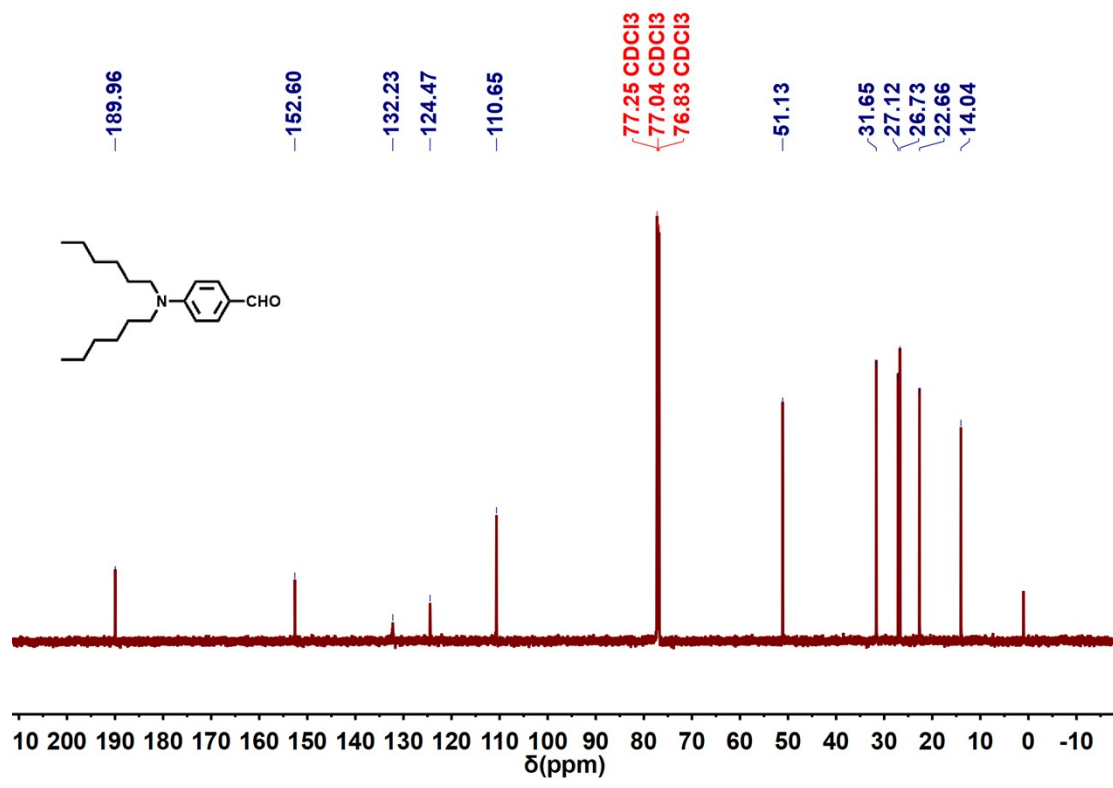
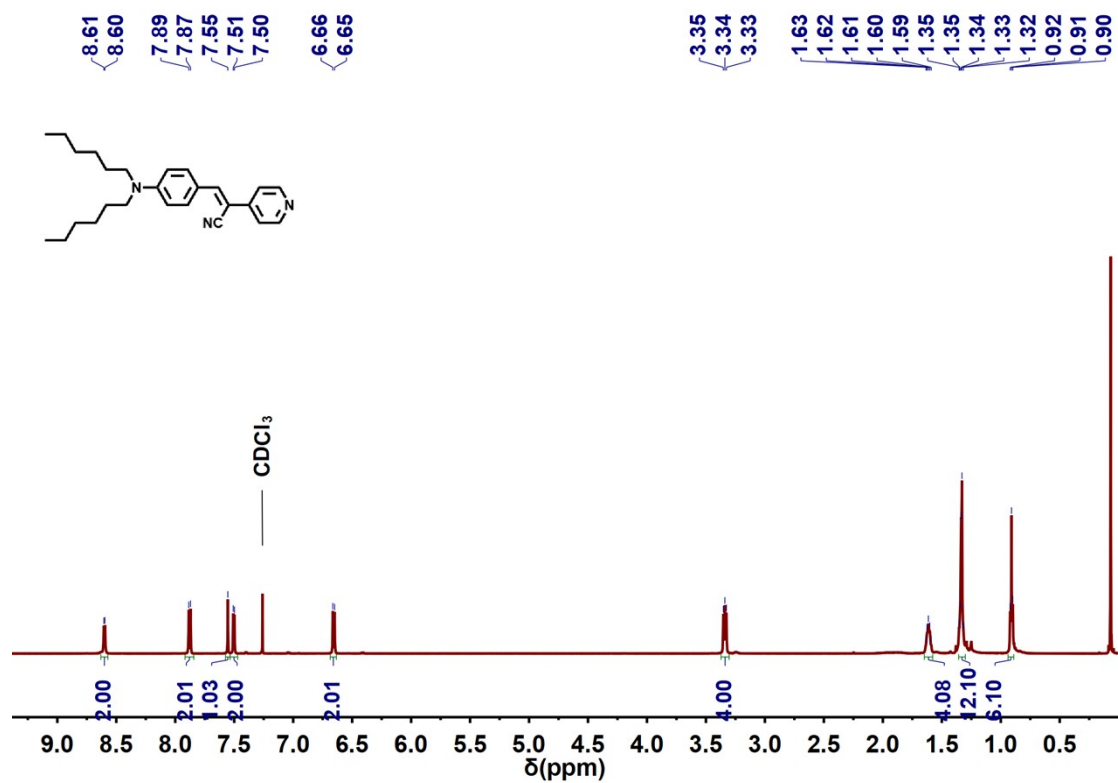
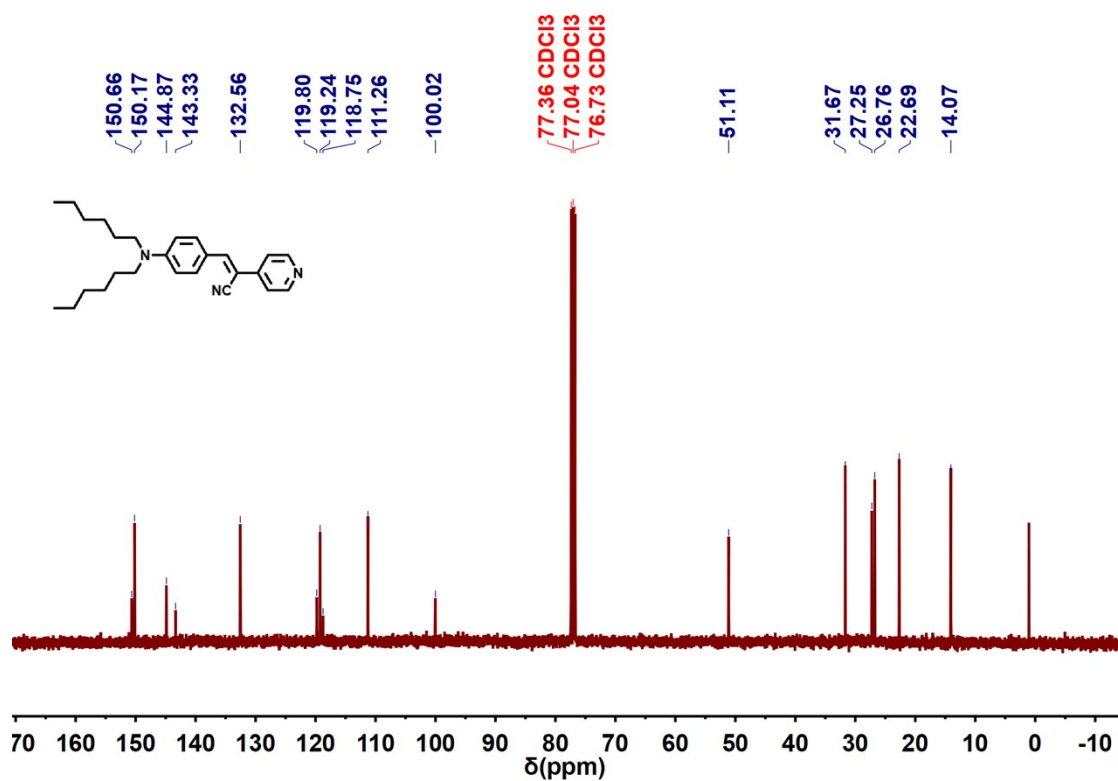


Figure S18. <sup>13</sup>C NMR spectra of 4-(dihexylamino)benzaldehyde (2) in CDCl<sub>3</sub>



**Figure S19.** <sup>1</sup>H NMR spectra of (Z)-3-(4-(dihexylamino)phenyl)-2-(pyridin-4-yl)acrylonitrile (3) in CDCl<sub>3</sub>



**Figure S20.** <sup>13</sup>C NMR spectra of (Z)-3-(4-(dihexylamino)phenyl)-2-(pyridin-4-yl)acrylonitrile (3) in CDCl<sub>3</sub>

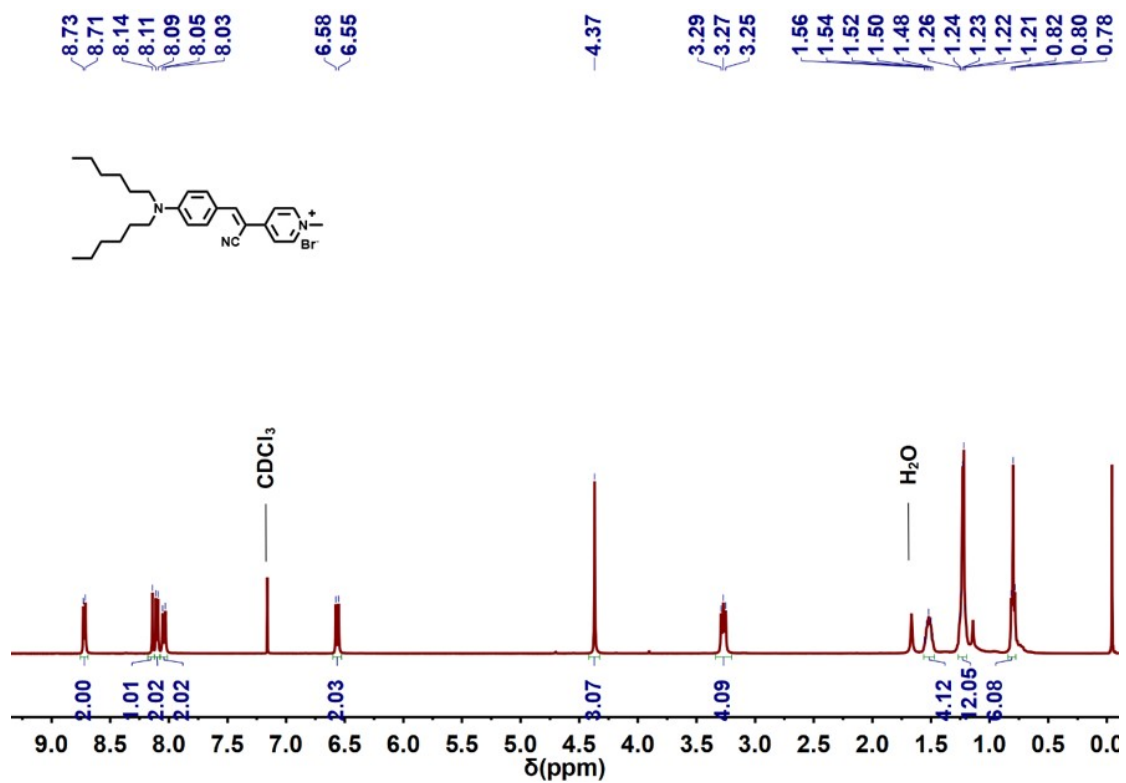


Figure S21. <sup>1</sup>H NMR spectra of CSP in CDCl<sub>3</sub>

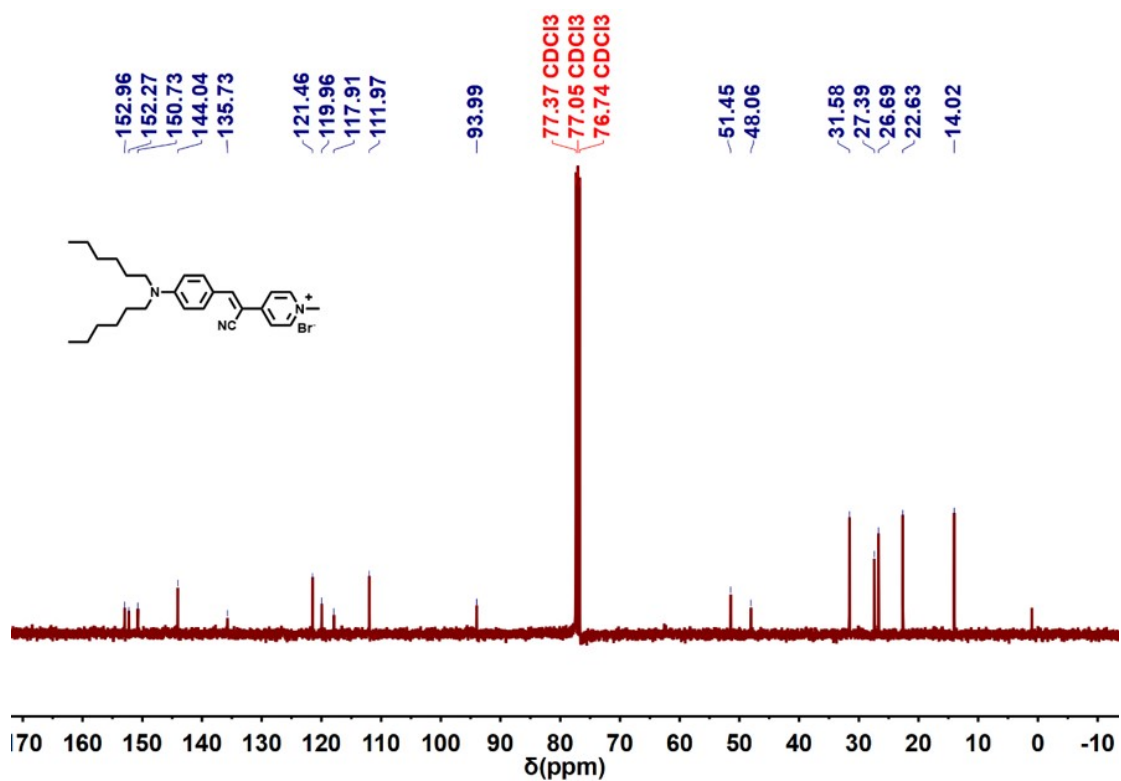


Figure S22. <sup>13</sup>C NMR spectra of CSP in CDCl<sub>3</sub>

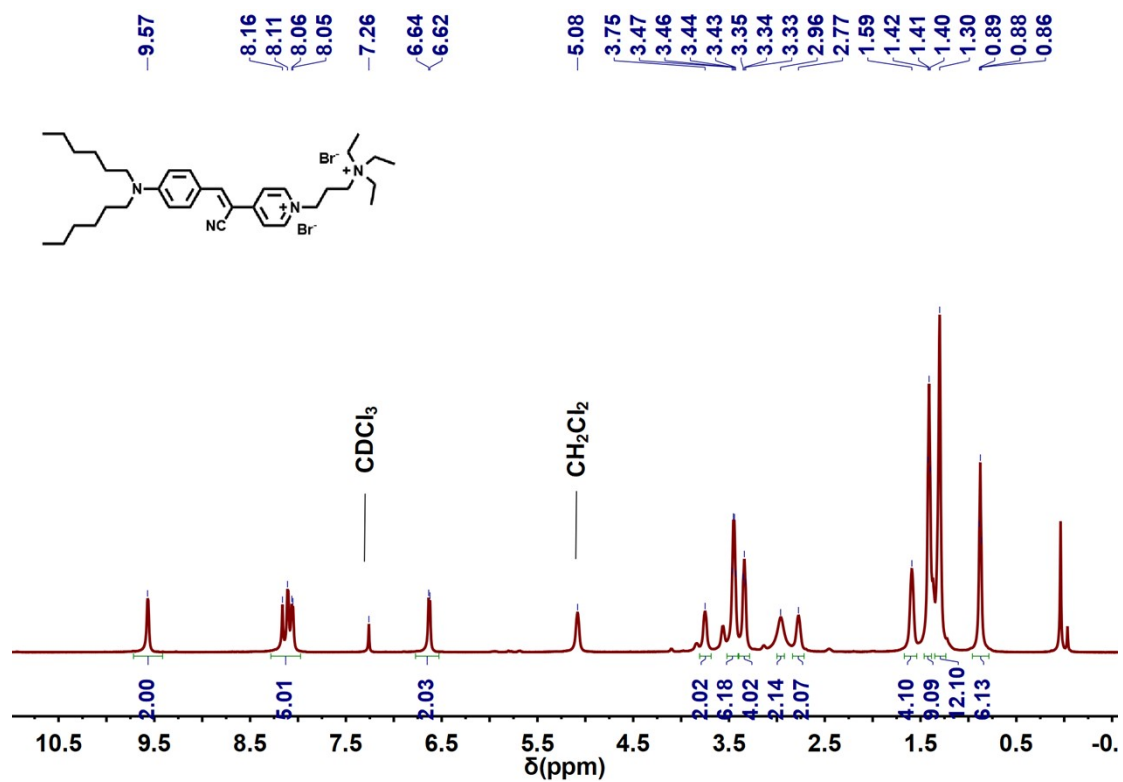


Figure S23.  $^1\text{H}$  NMR spectra of CSP-TEA in  $\text{CDCl}_3$

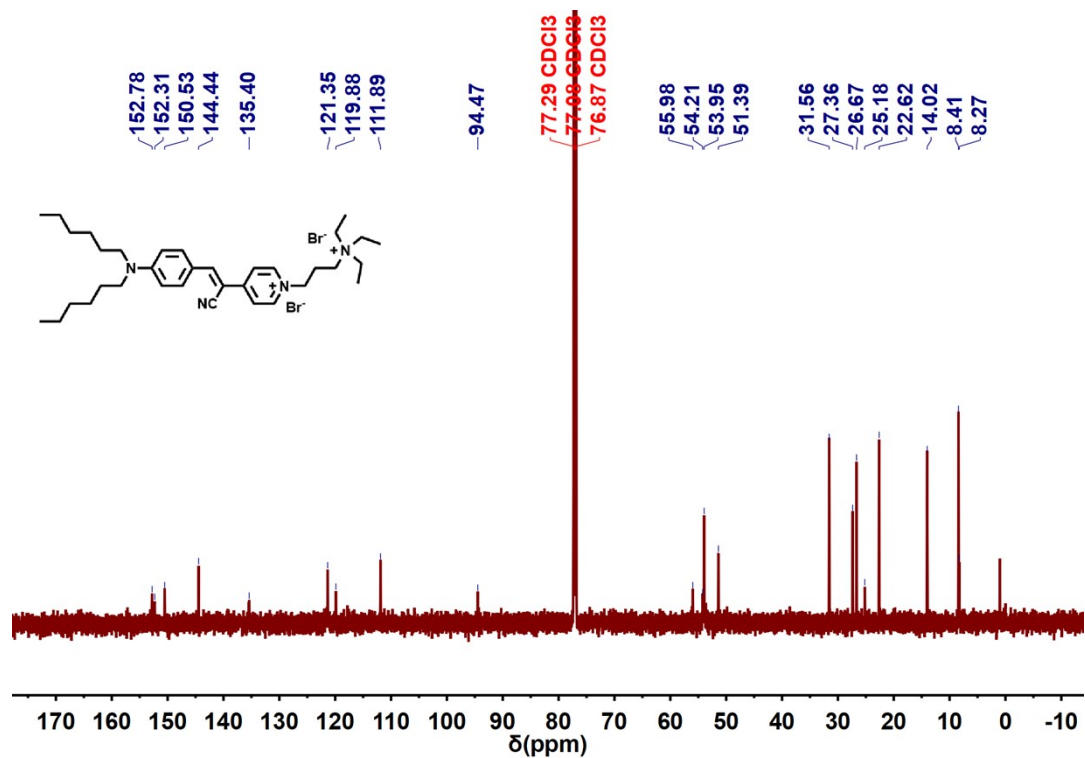


Figure S24.  $^{13}\text{C}$  NMR spectra of CSP-TEA in  $\text{CDCl}_3$

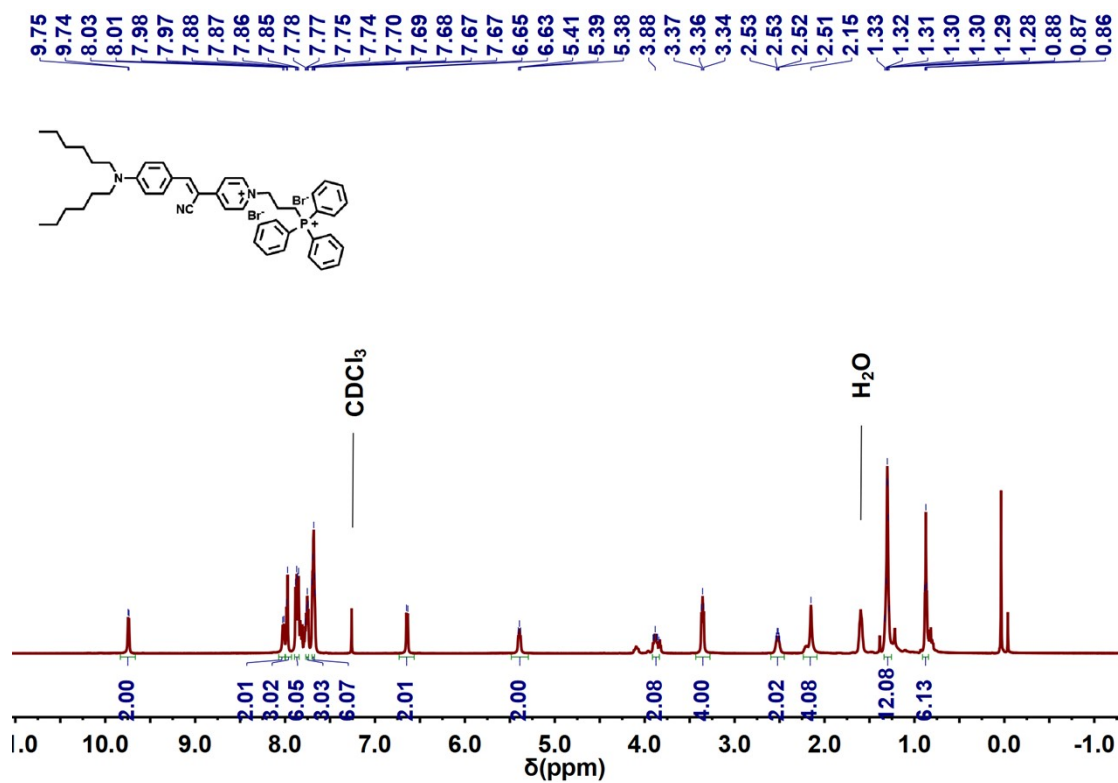


Figure S25.  $^1\text{H}$  NMR spectra of CSP-TPP in  $\text{CDCl}_3$

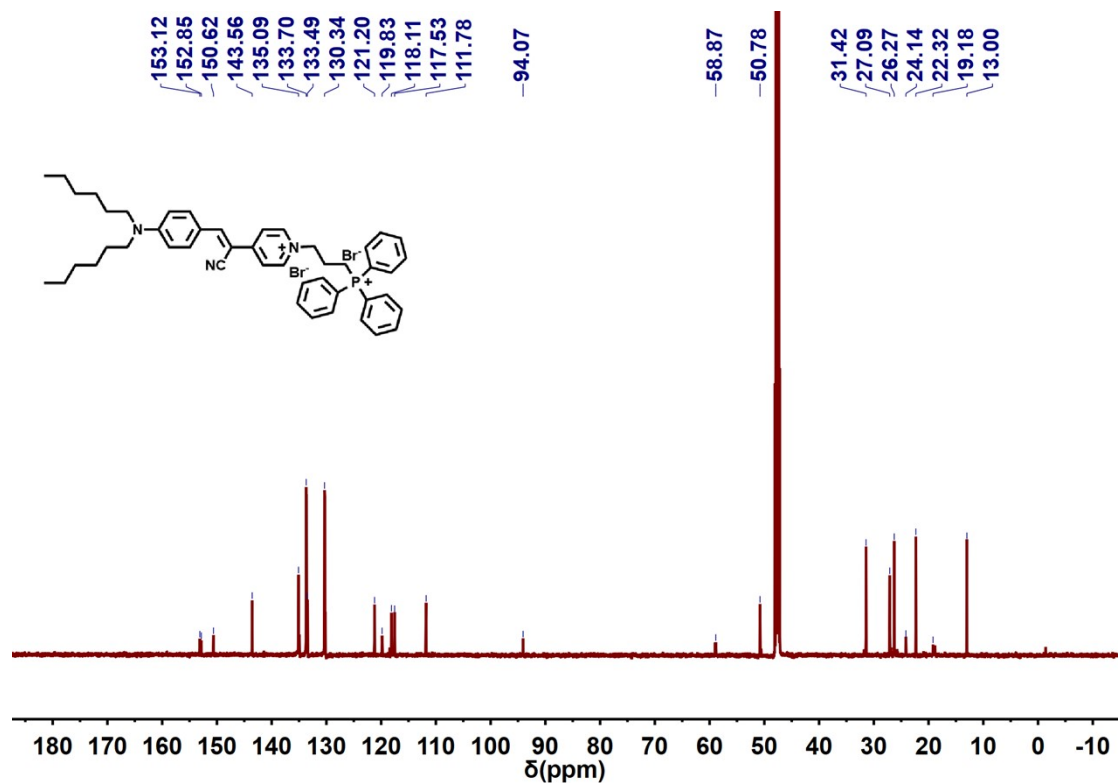


Figure S26.  $^{13}\text{C}$  NMR spectra of CSP-TPP in  $\text{CD}_3\text{OD}$

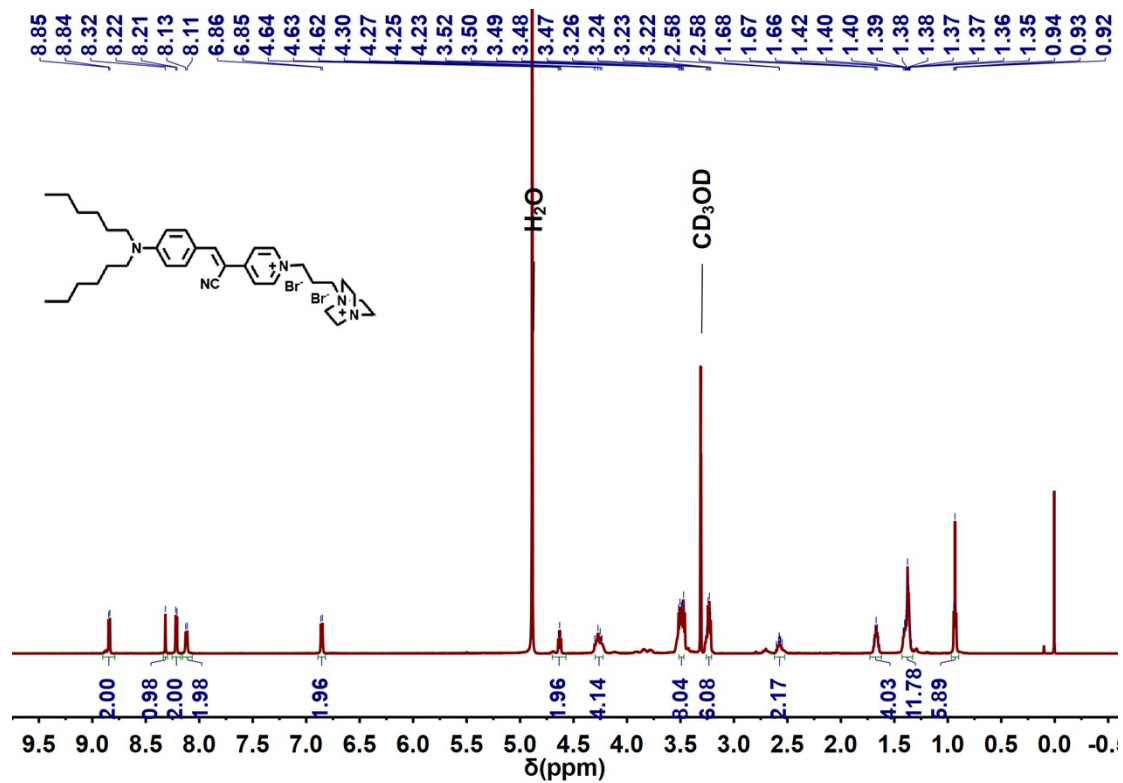


Figure S27.  $^1\text{H}$  NMR spectra of CSP-DBO in  $\text{CD}_3\text{OD}$

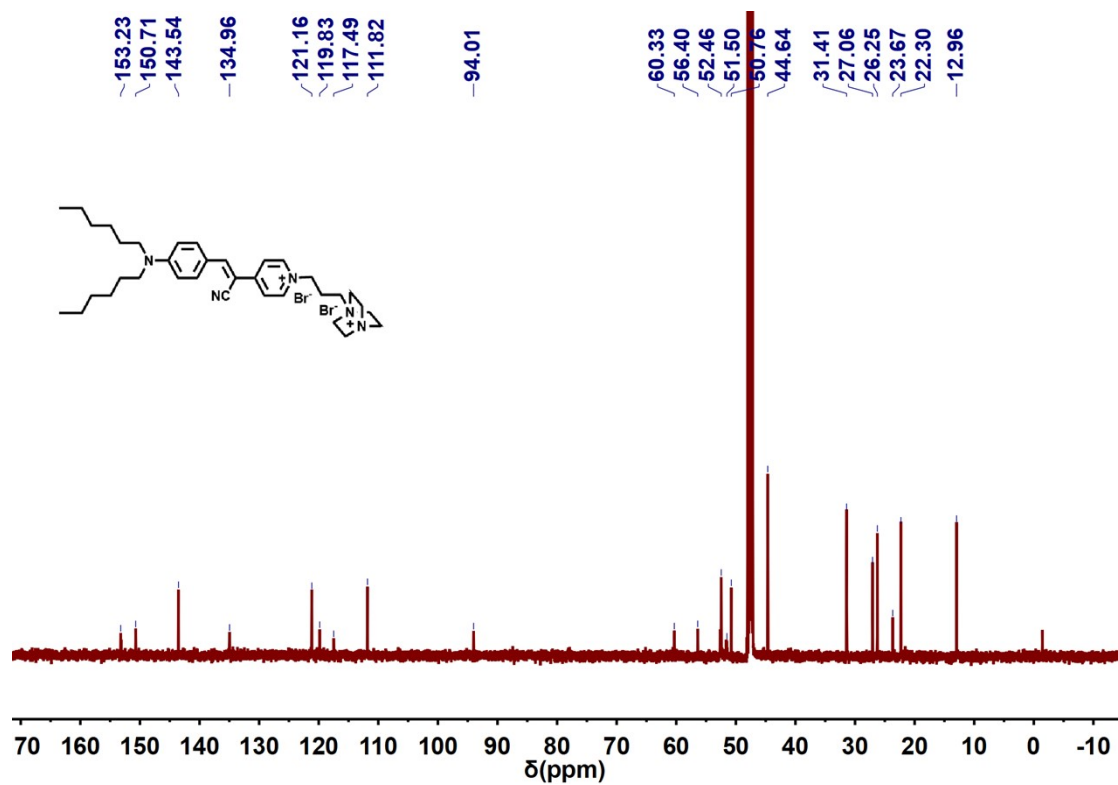


Figure S28.  $^{13}\text{C}$  NMR spectra of CSP-DBO in  $\text{CD}_3\text{OD}$



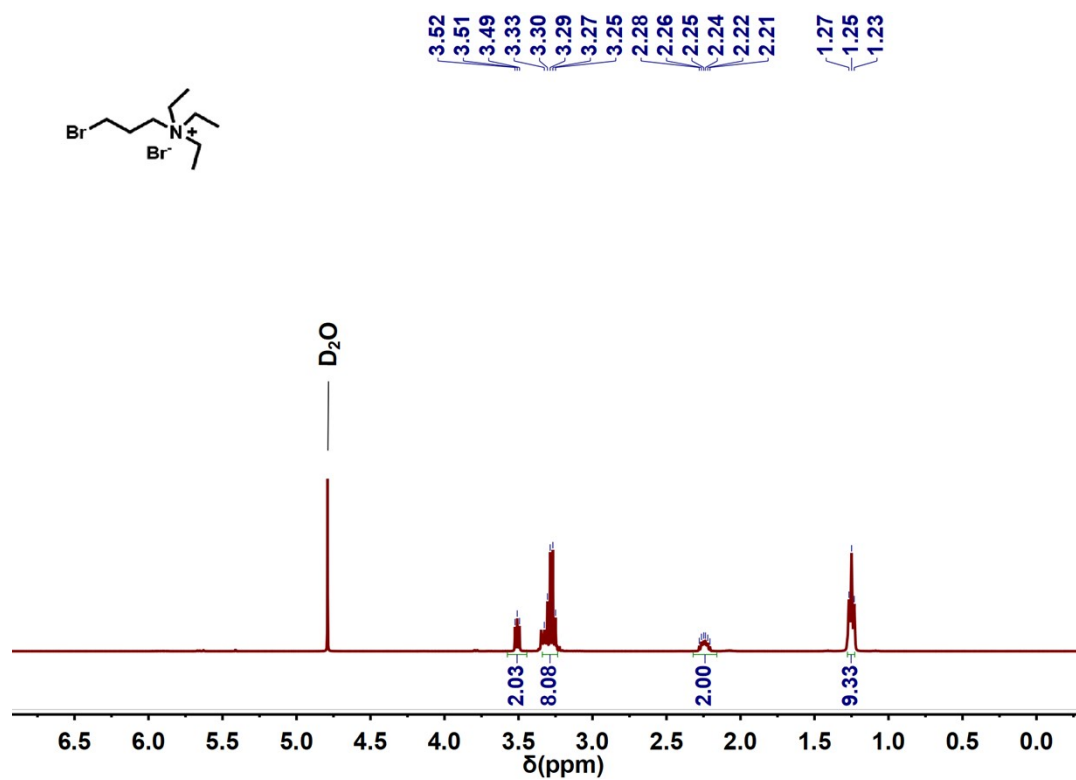


Figure S29.  $^1\text{H}$  NMR spectra of 3-bromo-N,N,N-triethylpropan-1-aminium in D<sub>2</sub>O

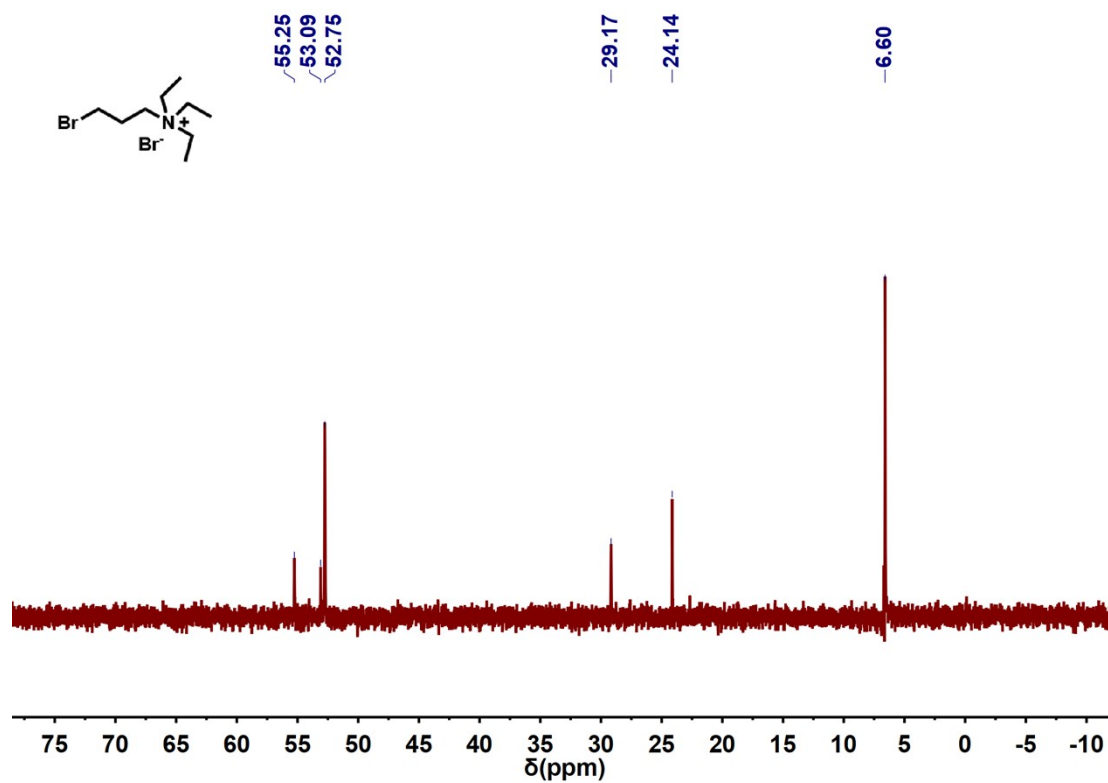


Figure S30.  $^{13}\text{C}$  NMR spectra of 3-bromo-N,N,N-triethylpropan-1-aminium in D<sub>2</sub>O

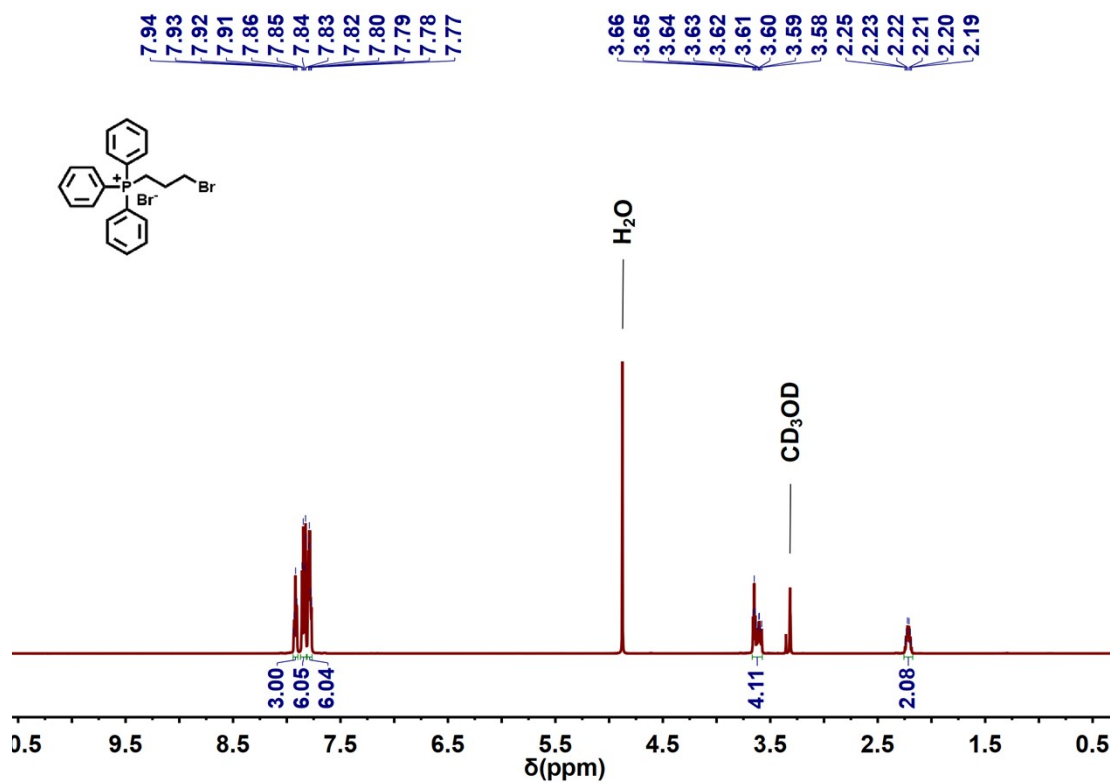


Figure S31.  $^1\text{H}$  NMR spectra of (3-bromopropyl)triphenylphosphonium in  $\text{CD}_3\text{OD}$

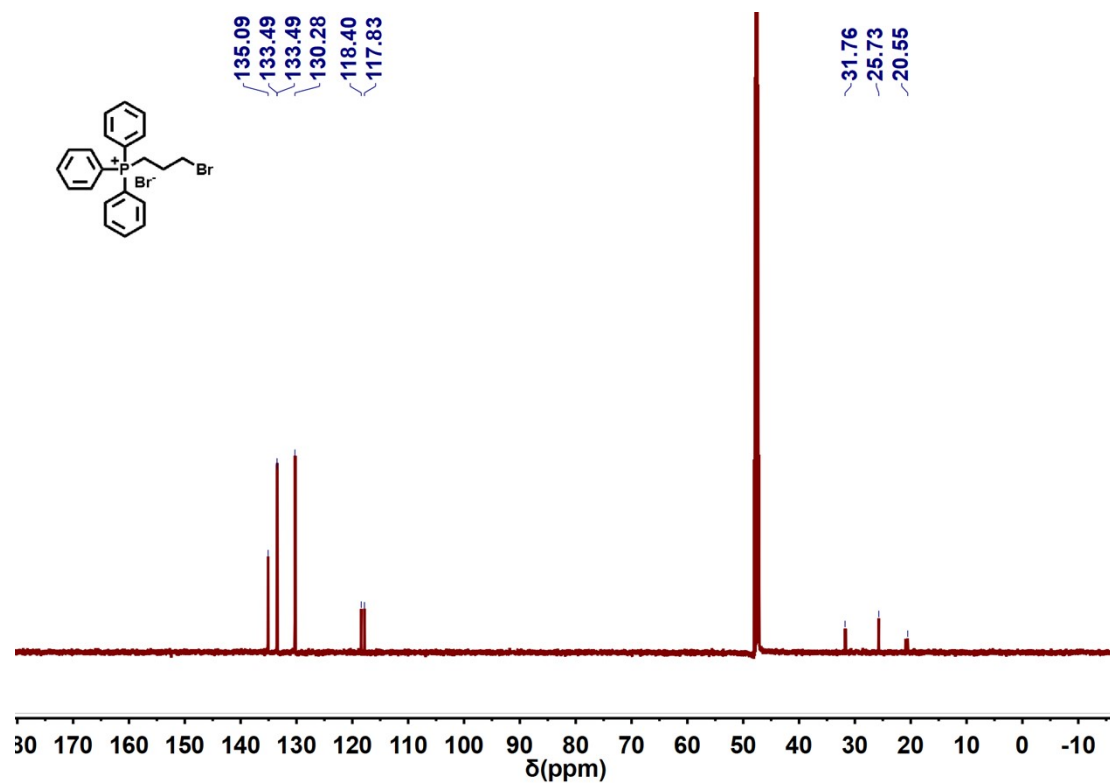
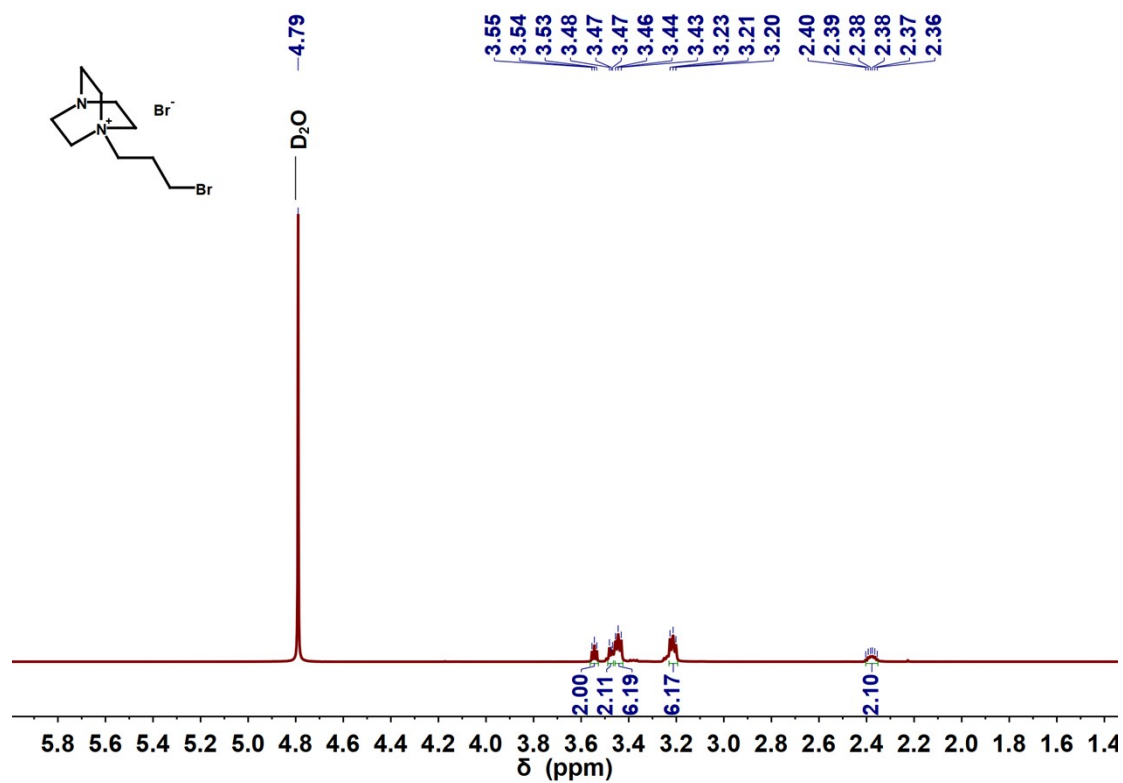
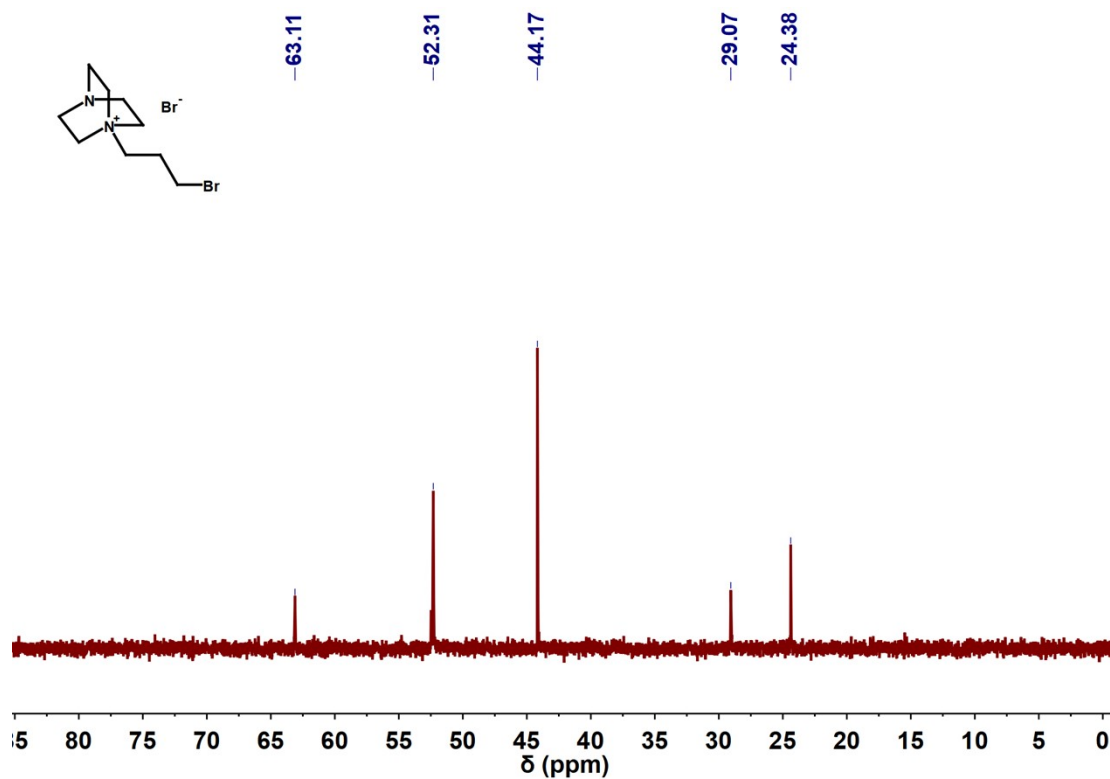


Figure S32.  $^{13}\text{C}$  NMR spectra of (3-bromopropyl)triphenylphosphonium in  $\text{CD}_3\text{OD}$



**Figure S33.**  $^1\text{H}$  NMR spectra of 1-(3-bromopropyl)-1,4-diazabicyclo[2.2.2]octan-1-ium in  $\text{D}_2\text{O}$



**Figure S34.**  $^{13}\text{C}$  NMR spectra of 1-(3-bromopropyl)-1,4-diazabicyclo[2.2.2]octan-1-ium in  $\text{D}_2\text{O}$

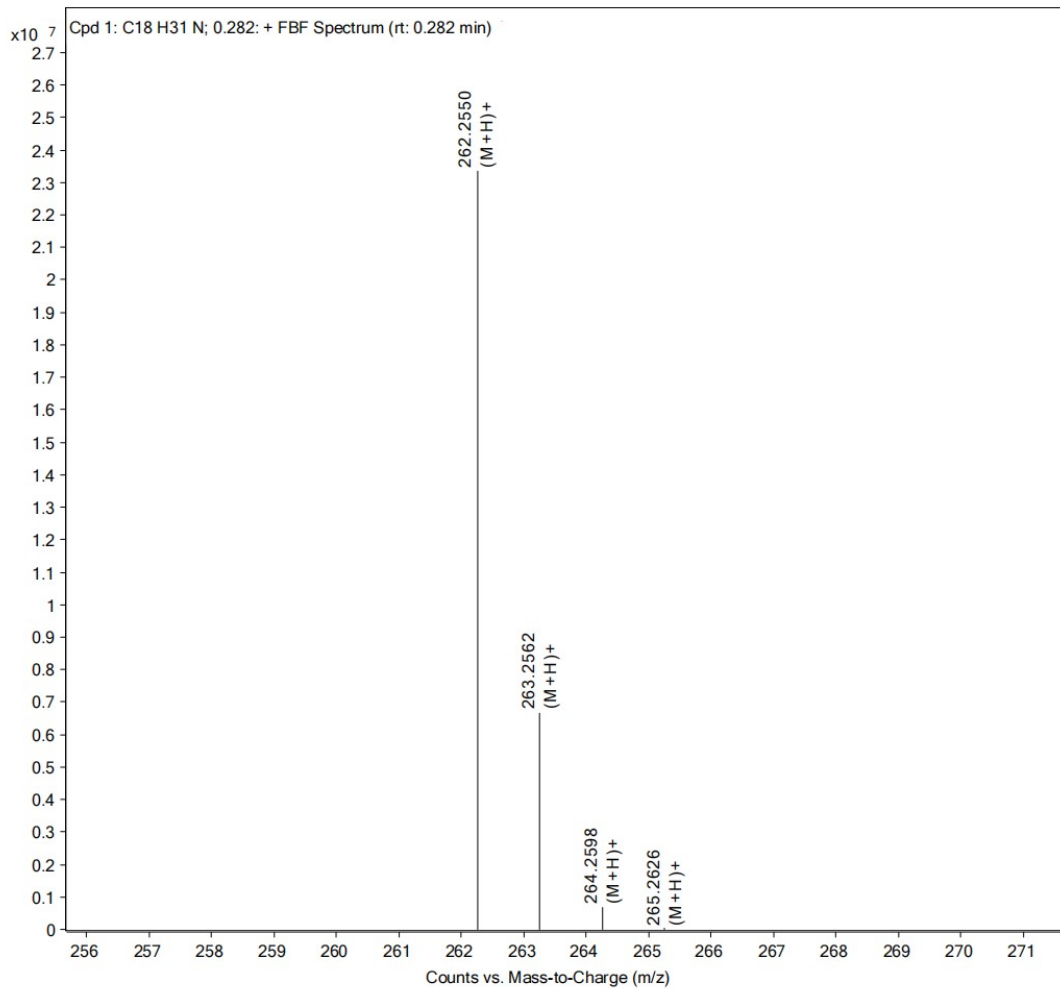


**Figure S35.** High-resolution mass spectrum of N,N-dihexylaniline (1)

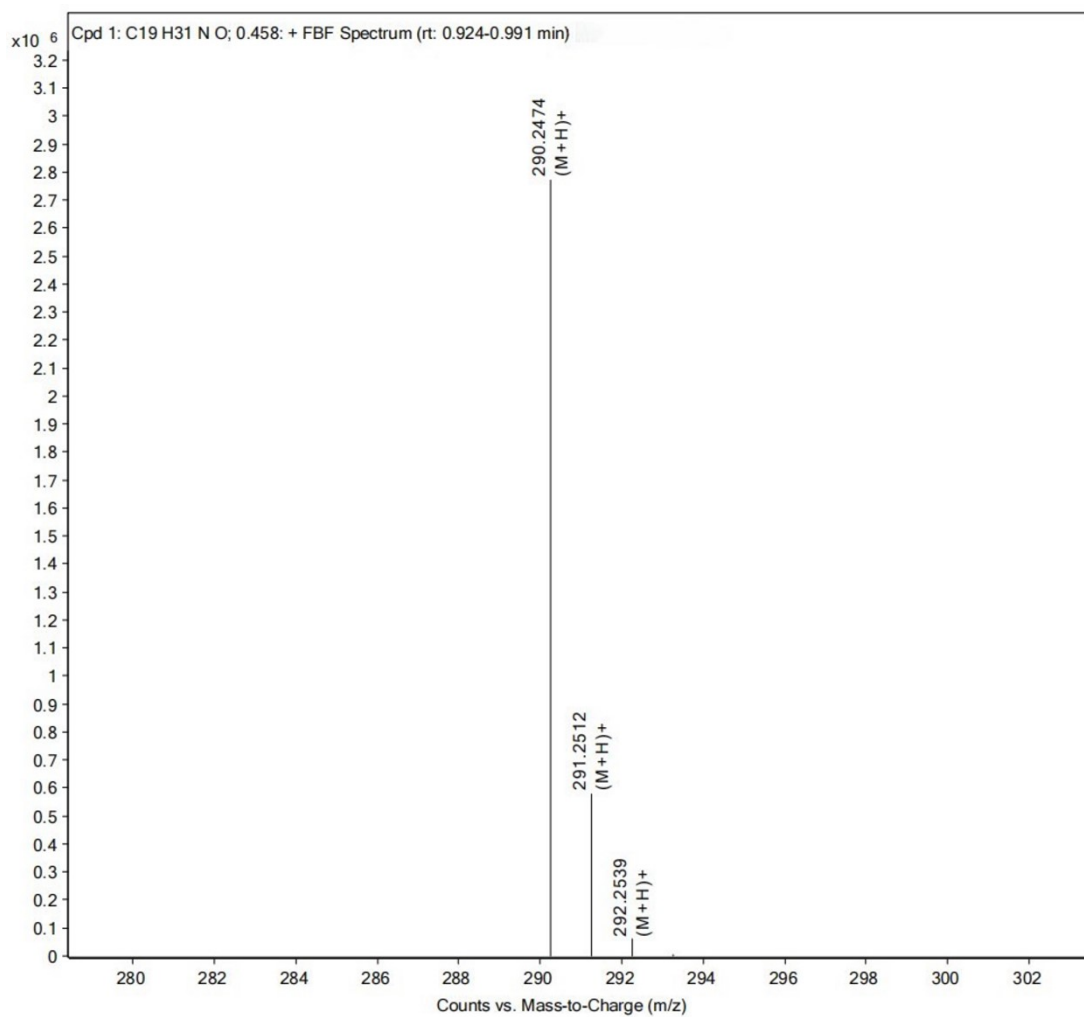


**Figure S36.** High-resolution mass spectrum of 4-(dihexylamino)benzaldehyde (2)

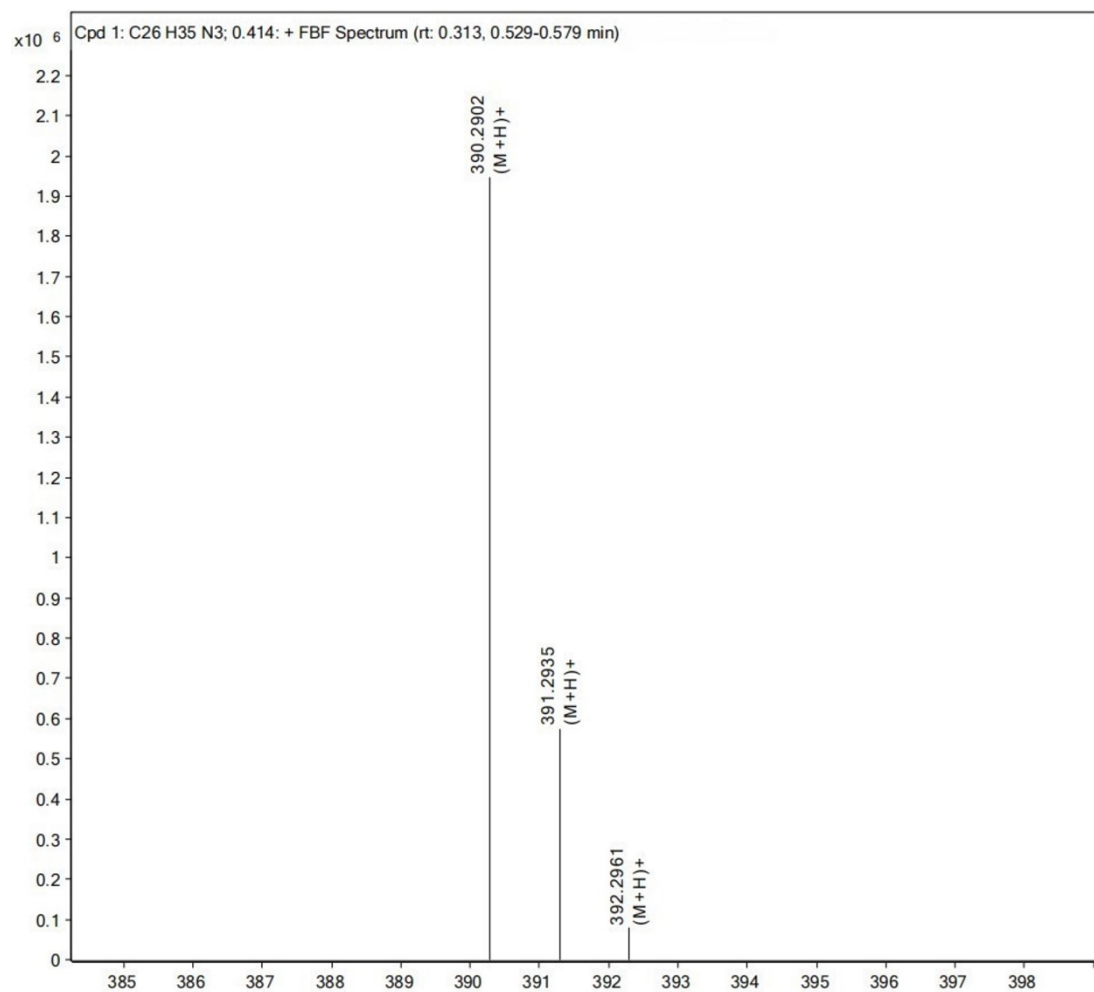


**Figure S37.** High-resolution mass spectrum of (Z)-3-(4-(dihexylamino)phenyl)-2-(pyridin-4-yl)acrylonitrile (3)

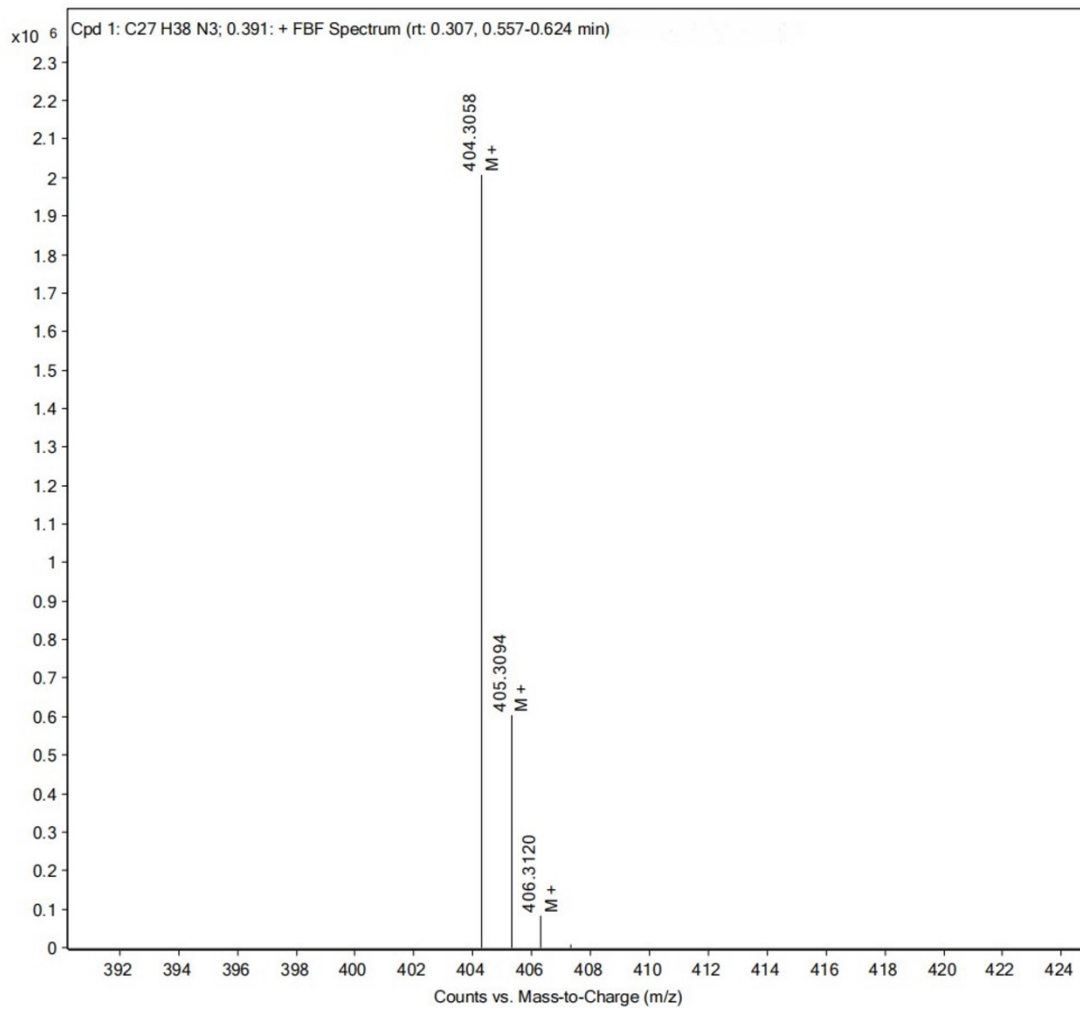


**Figure S38.** High-resolution mass spectrum of (Z)-4-(1-cyano-2-(4-(dihexylamino)phenyl)vinyl)-1-methylpyridin-1-ium iodide (CSP)

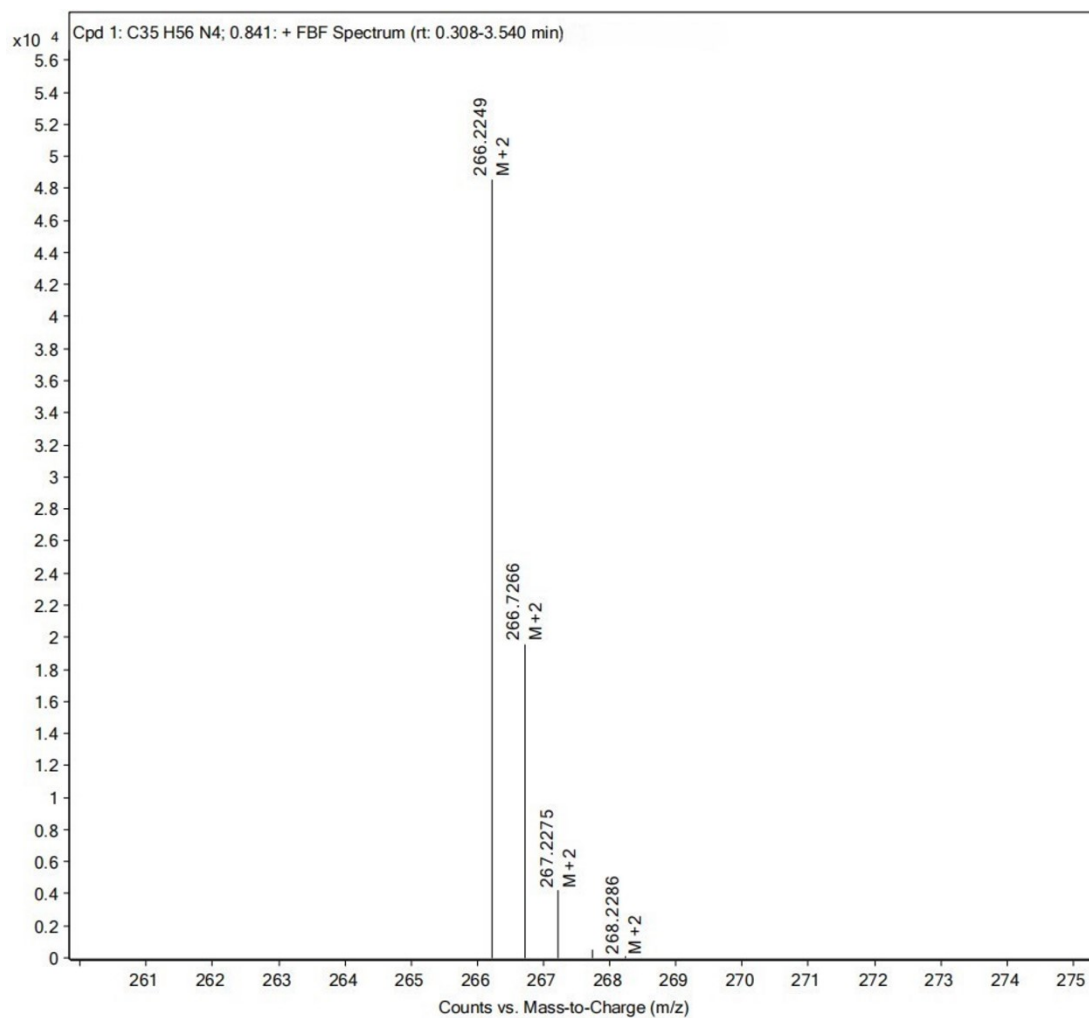


**Figure S39.** High-resolution mass spectrum of (Z)-4-(1-cyano-2-(4-(dihexylamino)phenyl)vinyl)-1-(3-(triethylammonio)propyl)pyridin-1-ium bromide (CSP-TEA)



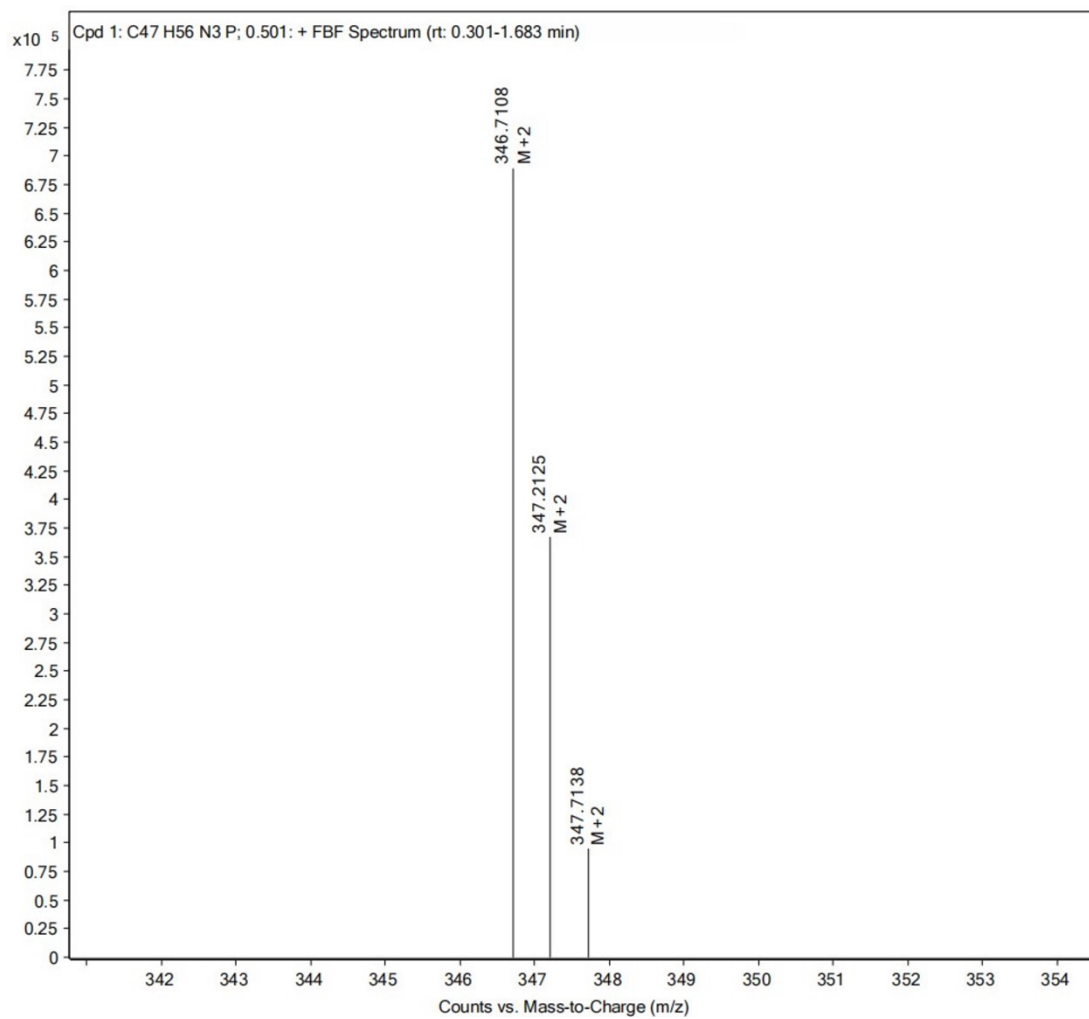


**Figure S40.** High-resolution mass spectrum of (Z)-4-(1-cyano-2-(4-(dihexylamino)phenyl)vinyl)-1-(3-(triphenylphosphonio)propyl)pyridin-1-ium bromide (CSP-TPP)

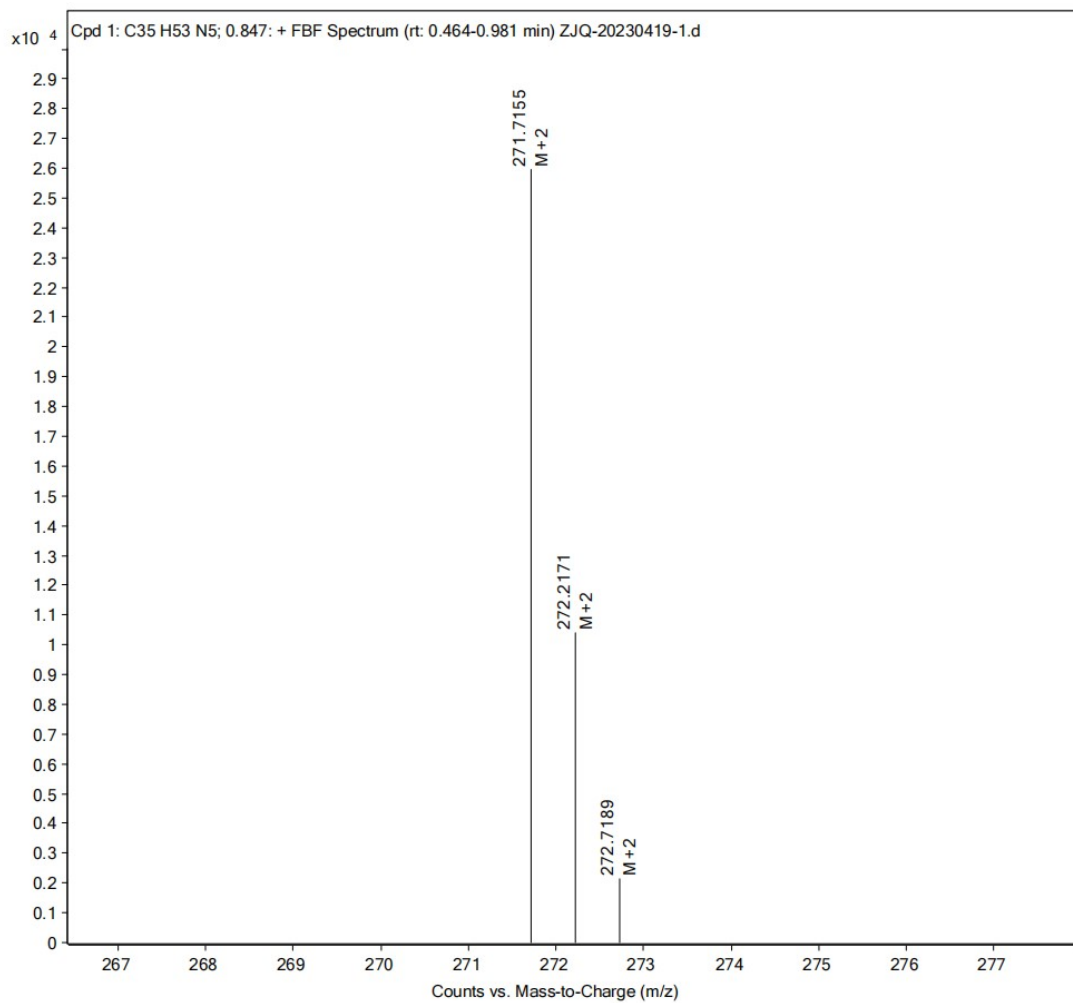


**Figure S41.** High-resolution mass spectrum of (Z)-1-(3-(4-(1-cyano-2-(4-(dihexylamino)phenyl)vinyl)pyridin-1-ium-1-yl)propyl)-1,4-diazabicyclo[2.2.2]octan-1-ium bromide (CSP-DBO)

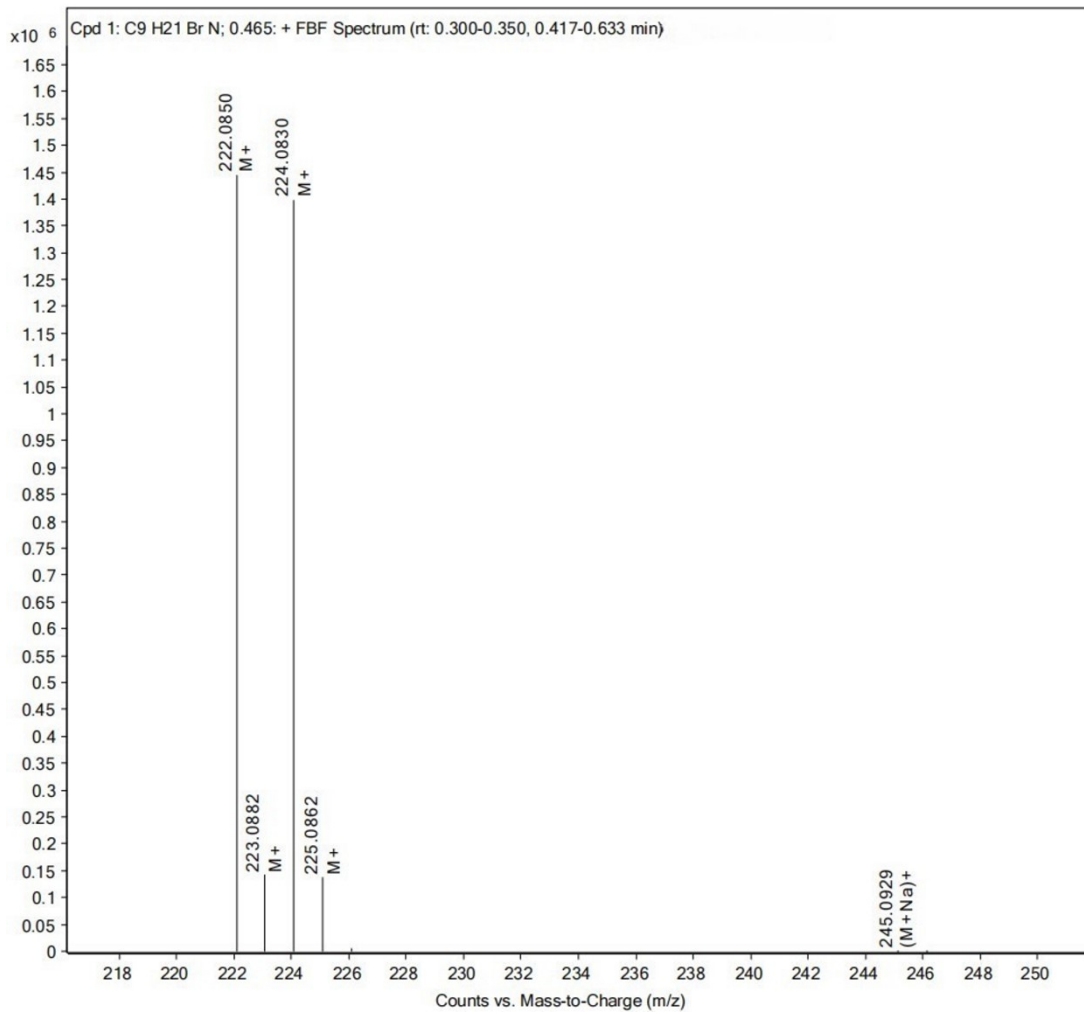


**Figure S42.** High-resolution mass spectrum of 3-bromo-N,N,N-triethylpropan-1-ammonium bromide

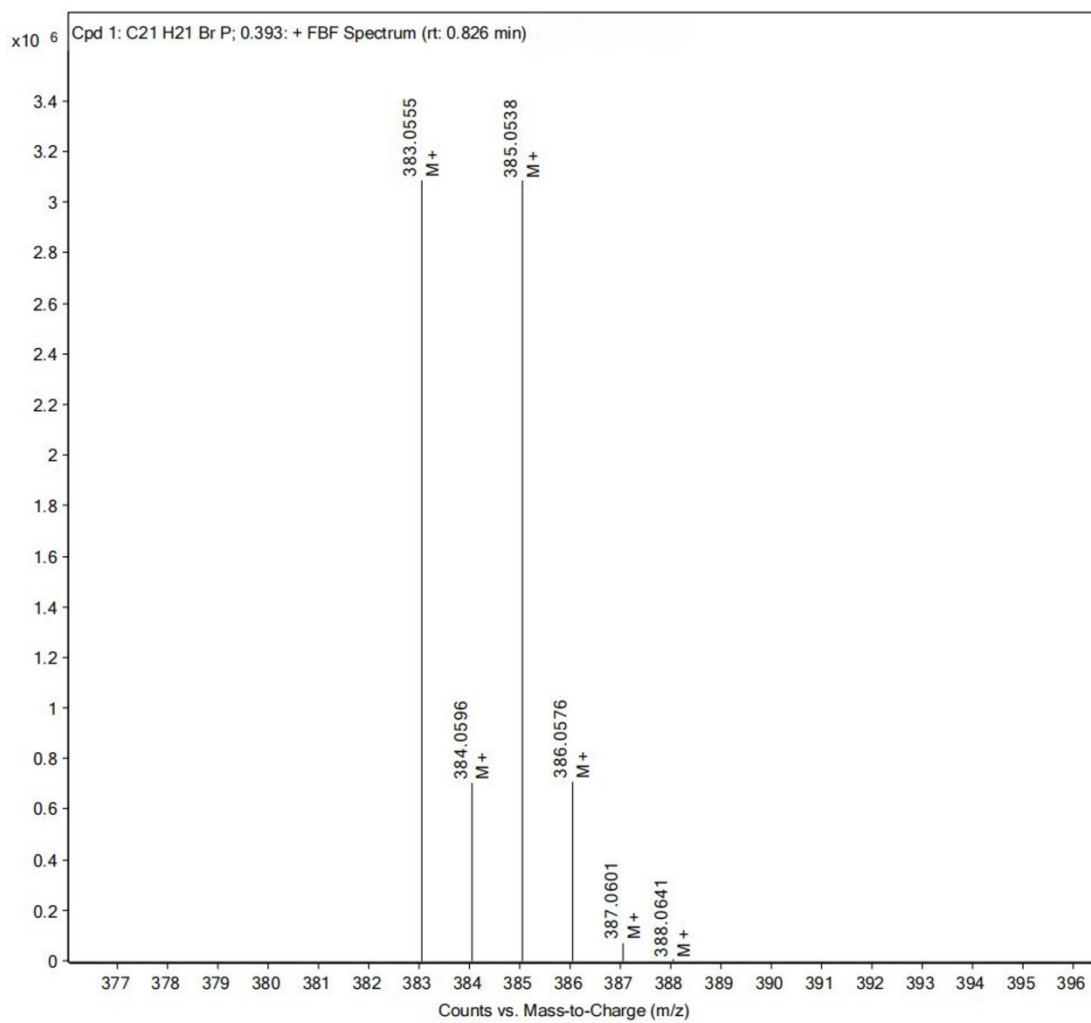


**Figure S43.** High-resolution mass spectrum of (3-bromopropyl)triphenylphosphonium bromide

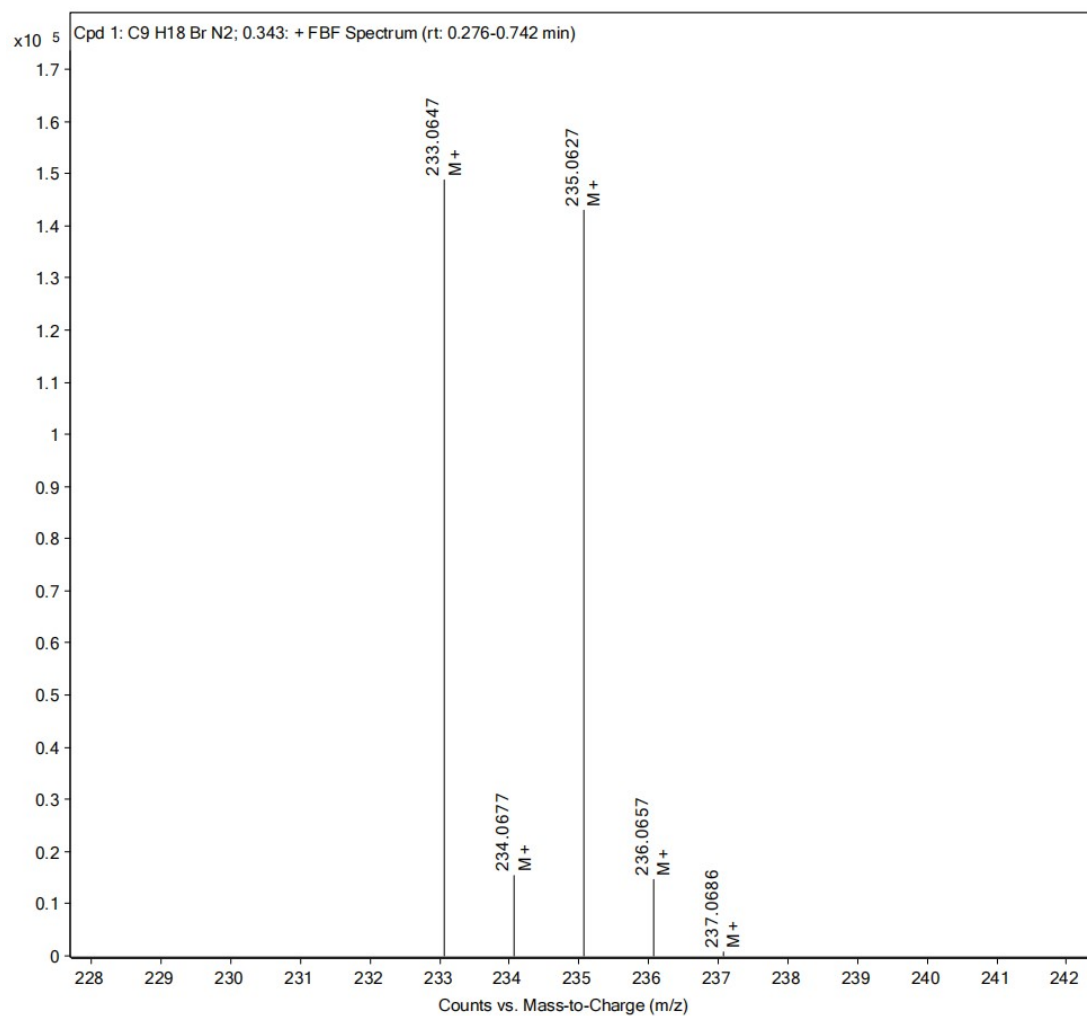


**Figure S44.** High-resolution mass spectrum of 1-(3-bromopropyl)-1,4-diazabicyclo[2.2.2]octan-1-ium bromide

## 5. REFERENCE

- [1] S. He, H. Gou, Y. Zhou, C. Wu, X. Ren, X. Wu, G. Guan, B. Jin, J. Huang, Z. Jin, T. Zhao, *The FASEB Journal*. **2023**, 37, e23269.